

7

Stress, Motion, and Constitutive Relations

7.1 Introduction

A fluid can be defined as any substance that flows under the action of a shear stress, no matter how small the shear. Alternatively, some define a fluid as any substance that quickly assumes the shape of the container in which it is placed. Regardless of the specific definition, common experience shows that materials in either their liquid or their gaseous phases can fall within the purview of fluid mechanics.

As noted in Chap. 1, biofluid mechanics is a very important field within biomedical engineering. For example, biofluid mechanics helps us to understand blood flow within the cardiovascular system, airflow within the airways and lungs, and the removal of waste products via the kidneys and urinary system. Biofluid mechanics is thus fundamental to understanding basic physiologic processes as well as clinical observations. We also know that the human body, and similarly each of its cells, consists largely of water (~70 %). Research over the last two decades has revealed that interstitial water in tissues and organs and, likewise, the cytosolic water in cells each play key roles in many biomechanical as well as biochemical processes. For example, the extensive water within the cartilage in articulating joints, such as the knee, carries a significant portion of the early compressive loading during standing, walking, and running. These tissues are porous, however, and the fluid can flow into or out of the tissues. Such fluid flow plays a key role in governing both the mechanical properties and many of the mechanotransduction mechanisms. Hence, again, biofluid mechanics is very important. Finally, biofluid mechanics is fundamental to the design of medical devices such as artificial hearts, ventricular-assist devices, heart valves, artificial arteries, mechanical ventilators, heart–lung machines, artificial kidneys, IV pumps, and so on. Exercise 7.1

asks you to brainstorm other medical devices that can be designed only with knowledge of biofluid mechanics.

In addition to its importance in the clinical setting, biofluid mechanics plays a key role in the research laboratory. One frequently finds fluids moving through tubes, pumps, valves, and so forth in the biomedical laboratory, with research varying from studies of the effects of pharmacologic agents on the behavior of the heart, kidney, or arteries to Earth-based studies of the effects of microgravity on gene expression in cells. Again, specific examples are manifold. Let us accept, therefore, that biofluid mechanics is essential to basic and applied research as well as to clinical care, and thus begin our study.

Just as in solid mechanics, we generally divide fluid mechanics into two general categories: statics and dynamics (cf. Fig. 1.4). In the former, we are interested only in the pressure distribution within the fluid; in the latter, we are generally interested in calculating both the pressure and the velocity *fields*, for from these we can compute any quantity of interest (e.g., normal and shear stresses, acceleration, and vorticity). Whether static or dynamic, to solve any problem in mechanics, we must, in general, address five classes of relations:

Kinematics: to compute velocities, accelerations, shear rates, and so forth.

Stresses and tractions: to quantify the intensity of forces acting over oriented areas.

Balance relations: to ensure the balance of mass, momentum, and energy.

Constitutive relations: to describe mathematically the behavior of the material.

Boundary/initial conditions: for mathematical and physical completeness.

Indeed, a review of our problem formulations in Part II reveals that we used these five classes of relations in most problems. Within this general five-step approach, there are multiple ways of formulating problems in biofluid mechanics: in terms of differential equations, which provide the most detail; in terms of integral equations, which provide gross or average information; and via semi-empirical methods that exploit the availability of particular data. We illustrate each approach in Chaps. 8–10.

7.2 Stress and Pressure

Recall from Chap. 2 that Euler and Cauchy first showed that the concept of stress is extremely useful in studying the mechanics of continua. In particular, depending on the application, one can define stress in various ways—the Cauchy stress $[\sigma]$, the first Piola–Kirchhoff stress $[\Sigma]$, or the second Piola–Kirchhoff stress $[S]$ as discussed in Chap. 6. Whereas each of these “measures” of stress is useful in nonlinear solid mechanics, experience has shown that Cauchy’s definition of stress is the most useful when studying the mechanics

of fluids whether they exhibit a linear or a nonlinear behavior. Recall from Chap. 2, therefore, that the *Cauchy stress is a measure of a force acting on an oriented area in the current configuration*. Moreover, because we can resolve any force that acts on a generic cube of material in terms of three components, the three orientations of the faces of the cube yield nine components of the Cauchy stress, which can be represented using a 3×3 matrix $[\sigma]$ at each point in general. Fortunately, only six of these components are independent due to the need to respect the balance of angular momentum.

Because our discussion of Cauchy stress in Chap. 2 was independent of the material or the deformation, everything holds equally well for a fluid. Hence, we will again be interested in components denoted as

$$\sigma_{(\text{face})(\text{direction})} \quad (7.1)$$

with respect to the coordinate system of interest [Eqs. (2.8)–(2.12)]. If needed, the stress transformation relations [Eqs. (2.13)–(2.21)] similarly hold.

In contrast to solid mechanics, however, the concept of pressure is particularly important in describing the mechanical behavior of fluids as well as in the solution of initial boundary value problems of interest. The *hydrostatic pressure* is defined herein as $-1/3$ of the sum of the diagonal components of the Cauchy stress when it is written in matrix form. For example, in Cartesians,

$$[\sigma] = \begin{bmatrix} \sigma_{xx} & \sigma_{xy} & \sigma_{xz} \\ \sigma_{yx} & \sigma_{yy} & \sigma_{yz} \\ \sigma_{zx} & \sigma_{zy} & \sigma_{zz} \end{bmatrix} \quad (7.2)$$

and thus the pressure p is given by

$$p = -\frac{1}{3}(\sigma_{xx} + \sigma_{yy} + \sigma_{zz}). \quad (7.3)$$

Because this combination of components is a coordinate invariant quantity (cf. Exercise 2.4), we equivalently have

$$p = -\frac{1}{3}(\sigma'_{xx} + \sigma'_{yy} + \sigma'_{zz}) \quad (7.4)$$

and similarly for cylindrical, sphericals, and other convenient coordinate systems. Pressure is thus a scalar field quantity, its value being independent of coordinate system. We will see in Sect. 7.4 that pressure and stress each play important roles in the constitutive formulation of a common class of fluid behaviors.

7.3 Kinematics: The Study of Motion

Let us next consider the motion of a fluid element in a flow field. For convenience, we follow an infinitesimal fluid element having a fixed identifiable mass Δm , which occupies a region $\Delta x \Delta y \Delta z$ in its current configuration (Fig. 7.1). As Δm moves in a flow field, several things may happen: It may translate, rotate, stretch, or shear. Although each of these motions may occur in three dimensions, it is useful to visualize them first in two dimensions. If the element translates (Fig. 7.2a), each particle undergoes the same displacement; for example, a particle at location (x_0, y_0, z_0) at time t_0 moves to a different location (x, y, z) , at any time t , and the associated displacement or velocity vector holds for all particles of Δm . If the element rotates, it again moves as a rigid body, but the particles do not experience the same displacement. Figure 7.2b shows a rotation of the element

FIGURE 7.1 Schema of a differential cube that defines a fluid element of mass $\rho \Delta x \Delta y \Delta z$, where ρ is the mass density. Whereas actual cubes of solid (like an ice cube) are convenient for study, this is merely a fictitious cube of fluid.

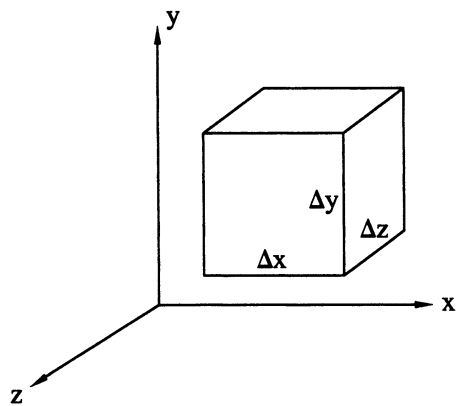
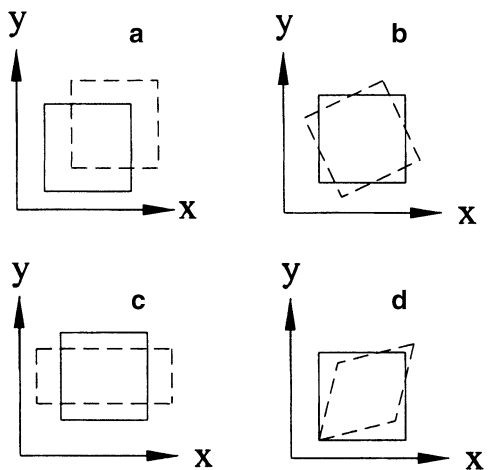


FIGURE 7.2 Four different types of motion (shown here in two dimensions for simplicity) that can be experienced by a fluid element: (a) a rigid-body translation, (b) a rigid-body rotation, (c) an extension, and (d) a pure shear.



about a z coordinate axis; clearly, the central particle does not change its location (x_0, y_0, z_0) , whereas all other particles do. In general, of course, the element may rotate about all three of the coordinate axes at the same time. In addition, the fluid element may deform or “strain.” Just as in solids, the deformation may be thought to consist of two types: changes in lengths (extensions) and changes in internal angles (shear). See Fig. 7.2c, d. In fluids, we are often interested in the (time) rate of change of the deformation, not just the displacements or their spatial gradients (i.e., strains). This will be discussed in detail below. In general, therefore, a fluid element may undergo a combination of translation, rotation, extension, and shear, all in three dimensions, during the course of its motion.

7.3.1 Velocity and Acceleration

Consider a particle located at (x, y, z) at time t . Its position vector, relative to an origin at $(0, 0, 0)$, is $\mathbf{x} = x(t)\hat{\mathbf{i}} + y(t)\hat{\mathbf{j}} + z(t)\hat{\mathbf{k}}$ with respect to a Cartesian coordinate system. Velocity is defined as the rate of change of position. Hence, we have

$$\mathbf{v} = \frac{d\mathbf{x}}{dt} = \frac{dx}{dt}\hat{\mathbf{i}} + \frac{dy}{dt}\hat{\mathbf{j}} + \frac{dz}{dt}\hat{\mathbf{k}}. \quad (7.5)$$

Because velocity is a vector,¹ it can be written as

$$\mathbf{v} = v_x\hat{\mathbf{i}} + v_y\hat{\mathbf{j}} + v_z\hat{\mathbf{k}} \quad (7.6)$$

with respect to a Cartesian coordinate system. If so, its Cartesian components are simply

$$v_x = \frac{dx}{dt}, \quad v_y = \frac{dy}{dt}, \quad v_z = \frac{dz}{dt}. \quad (7.7)$$

Similarly, relative to a cylindrical coordinate system, one can have²

$$\mathbf{v} = v_r\hat{\mathbf{e}}_r + v_\theta\hat{\mathbf{e}}_\theta + v_z\hat{\mathbf{e}}_z. \quad (7.8)$$

The primary difference between the Cartesian and cylindrical representations is that the Cartesian bases $(\hat{\mathbf{i}}, \hat{\mathbf{j}}, \hat{\mathbf{k}})$ do not change with position, whereas two of the cylindrical bases $(\hat{\mathbf{e}}_r, \hat{\mathbf{e}}_\theta, \hat{\mathbf{e}}_z)$ do change with position; that is, the directions of

¹ We shall make extensive use of vectors in our discussion of fluids. A brief review is in Appendix 7.

² For consistency, we could let $\hat{\mathbf{i}} \equiv \hat{\mathbf{e}}_x$, $\hat{\mathbf{j}} \equiv \hat{\mathbf{e}}_y$, and $\hat{\mathbf{k}} \equiv \hat{\mathbf{e}}_z$ in Eq. (7.6).

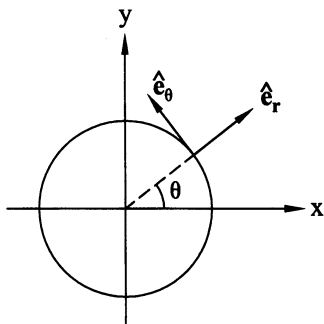


FIGURE 7.3 Illustration of the base vectors for a cylindrical-polar coordinate system. The direction of \hat{e}_r changes with changes in θ and so too for the direction of \hat{e}_θ . It is for this reason that spatial gradients of these base vectors need not be zero, in contrast to the case of Cartesian bases. This difference proves to be important in the derivation of many equations in biofluids because of the cylindrical shape of many conducting tubes (e.g., arteries, airways, and ureters).

\hat{e}_r and \hat{e}_θ change with θ (Fig. 7.3). This will prove important below, when velocity gradients are calculated.

Acceleration is simply the rate of change of velocity, but there are two ways of computing the acceleration. The most natural way is to take the time derivative of Eq. (7.5) (and similarly for cylindricals and other coordinate systems); that is,

$$\mathbf{a} = \frac{d\mathbf{v}}{dt} = \frac{d^2x}{dt^2}\hat{\mathbf{i}} + \frac{d^2y}{dt^2}\hat{\mathbf{j}} + \frac{d^2z}{dt^2}\hat{\mathbf{k}}. \quad (7.9)$$

Because acceleration is also a vector, we have

$$\mathbf{a} = a_x\hat{\mathbf{i}} + a_y\hat{\mathbf{j}} + a_z\hat{\mathbf{k}}; \quad (7.10)$$

thus, the Cartesian components are

$$a_x = \frac{d^2x}{dt^2}, \quad a_y = \frac{d^2y}{dt^2}, \quad a_z = \frac{d^2z}{dt^2}. \quad (7.11)$$

This approach for computing \mathbf{a} is common in solid mechanics and rigid-body dynamics; it is usually called a Lagrangian formulation. A prime example in rigid-body dynamics would be the calculation of the acceleration of a baseball after it leaves the bat; one only needs to know the (x, y, z) position of the mass center of the ball at each time as you “follow it” over the fence. Recall, too, that in solid mechanics, it is often useful to define the displacement vector $\mathbf{u}(t)$ as the difference between where we (a material point) are and where we were, namely

$$\mathbf{u}(t) = [x(t) - x(0)]\hat{\mathbf{i}} + [y(t) - y(0)]\hat{\mathbf{j}} + [z(t) - z(0)]\hat{\mathbf{k}}, \quad (7.12)$$

from which the acceleration can alternatively be computed as

$$\mathbf{a} = \frac{d^2u_x}{dt^2}\hat{\mathbf{i}} + \frac{d^2u_y}{dt^2}\hat{\mathbf{j}} + \frac{d^2u_z}{dt^2}\hat{\mathbf{k}}. \quad (7.13)$$

Equations (7.11) and (7.13) are equivalent because the original positions $x(0)$, $y(0)$, $z(0)$ at time $t=0$ do not change with time.

A second approach for computing acceleration arises if we recognize that the velocity \mathbf{v} is a field quantity (i.e., rather than following a single particle at each time t , we compute/measure \mathbf{v} at each point \mathbf{x} and each time t). For example, in Cartesians, we recognize that, in general,

$$\mathbf{v} = \mathbf{v}(x, y, z, t), \quad (7.14)$$

for which we must use the chain rule to compute the time derivative:

$$\mathbf{a} = \frac{d\mathbf{v}}{dt} = \frac{\partial \mathbf{v}}{\partial t} \frac{dt}{dt} + \frac{\partial \mathbf{v}}{\partial x} \frac{dx}{dt} + \frac{\partial \mathbf{v}}{\partial y} \frac{dy}{dt} + \frac{\partial \mathbf{v}}{\partial z} \frac{dz}{dt}. \quad (7.15)$$

From Eq. (7.7), therefore, the acceleration becomes

$$\mathbf{a} = \frac{\partial \mathbf{v}}{\partial t} + v_x \frac{\partial \mathbf{v}}{\partial x} + v_y \frac{\partial \mathbf{v}}{\partial y} + v_z \frac{\partial \mathbf{v}}{\partial z}, \quad (7.16)$$

or, in more compact notation,

$$\mathbf{a} = \frac{\partial \mathbf{v}}{\partial t} + (\mathbf{v} \cdot \nabla)\mathbf{v}, \quad (7.17)$$

where $\partial \mathbf{v} / \partial t$ is called the *local* acceleration and $(\mathbf{v} \cdot \nabla)\mathbf{v}$ is called the *convective* acceleration. A very important definition in fluids is that of a *steady flow*: A flow is said to be steady if $\partial \mathbf{v} / \partial t = \mathbf{0}$ (i.e., if there is no local acceleration). Of course, in Cartesians, the del operator ∇ can be written as³

$$\nabla = \hat{\mathbf{i}} \frac{\partial}{\partial x} + \hat{\mathbf{j}} \frac{\partial}{\partial y} + \hat{\mathbf{k}} \frac{\partial}{\partial z}. \quad (7.18)$$

³ Because ∇ is a differential operator, we remember that it operates on quantities to its right to form a gradient $\nabla \phi$ of a scalar ϕ , divergence $\nabla \cdot \mathbf{v}$ of a vector \mathbf{v} , or curl $\nabla \times \mathbf{v}$ of a vector.

Before continuing, it is instructive to show that Eqs. (7.16) and (7.17) are indeed equivalent. Given Eq. (7.16), we can factor out the common term, \mathbf{v} , leaving us with

$$\mathbf{a} = \frac{\partial \mathbf{v}}{\partial t} + \left(v_x \frac{\partial}{\partial x} + v_y \frac{\partial}{\partial y} + v_z \frac{\partial}{\partial z} \right) \mathbf{v}. \quad (7.19)$$

Now, resolving each term in the parentheses into its vector components, we are left with

$$\mathbf{a} = \frac{\partial \mathbf{v}}{\partial t} + \left[(v_x \hat{\mathbf{i}} + v_y \hat{\mathbf{j}} + v_z \hat{\mathbf{k}}) \cdot \left(\hat{\mathbf{i}} \frac{\partial}{\partial x} + \hat{\mathbf{j}} \frac{\partial}{\partial y} + \hat{\mathbf{k}} \frac{\partial}{\partial z} \right) \right] \mathbf{v}, \quad (7.20)$$

whereby we arrive at Eq. (7.17),

$$\mathbf{a} = \frac{\partial \mathbf{v}}{\partial t} + (\mathbf{v} \cdot \nabla) \mathbf{v}. \quad (7.21)$$

In so doing, note that $\mathbf{v} \cdot \nabla \neq \nabla \cdot \mathbf{v}$ because the former yields a differential operator and the latter a scalar value. Finally, recognizing that \mathbf{a} is a vector, Cartesian components are thus

$$\begin{aligned} a_x &= \frac{\partial v_x}{\partial t} + v_x \frac{\partial v_x}{\partial x} + v_y \frac{\partial v_x}{\partial y} + v_z \frac{\partial v_x}{\partial z}, \\ a_y &= \frac{\partial v_y}{\partial t} + v_x \frac{\partial v_y}{\partial x} + v_y \frac{\partial v_y}{\partial y} + v_z \frac{\partial v_y}{\partial z}, \\ a_z &= \frac{\partial v_z}{\partial t} + v_x \frac{\partial v_z}{\partial x} + v_y \frac{\partial v_z}{\partial y} + v_z \frac{\partial v_z}{\partial z}. \end{aligned} \quad (7.22)$$

This approach for computing acceleration is often adopted in fluid mechanics; it is called an Eulerian approach. In contrast to the aforementioned *Lagrangian approach* in which we follow material particles at different times, in the *Eulerian approach* we “watch” what happens to particles that go through multiple fixed points in space. A simple example that illustrates these approaches is to watch snowflakes fall while driving a car at night. One can either watch a particular snowflake approach the car and flow over the hood and past the windshield (a Lagrangian approach) or one could focus on a point in space and watch what happens to all the snowflakes that go through the point of interest (an Eulerian approach). The latter approach would typically be adopted by a fluid mechanicist and repeated at multiple points of interest to quantify the entire flow field $\mathbf{v} = \mathbf{v}(x, y, z, t)$. From Eq. (7.17), we recognize that a fluid particle moving in a flow field may accelerate for either of two reasons. For example, a fluid particle accelerates or decelerates if it is forced by an unsteady

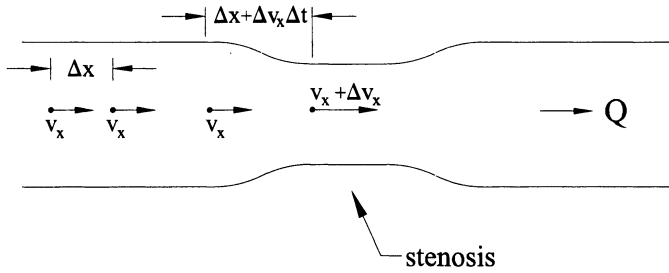


FIGURE 7.4 Schematic drawing of a stenosis (i.e., local narrowing) within a blood vessel. Stenoses often arise due to atherosclerosis, but other causes exist as well (e.g., extravascular blood due to a subarachnoid hemorrhage will cause a local vasospasm, whereas a local trauma due to a crushing injury or the overaggressive use of a vascular clamp during surgery can damage the vessel). Clearly, a fluid particle within the narrowed region will travel at a greater velocity than one in the inlet region; thus, the particles may accelerate as they enter the constriction despite no “time-dependent” change in the velocity.

source (e.g., a pulsatile pump like the heart). This is a local acceleration. Alternatively, a fluid particle accelerates if it flows through a constriction even if acted upon by an unchanging force (e.g., gravity flow through a funnel or venous flow through a stenotic valve). See Fig. 7.4. In this case, the particle is accelerated because it is convected to a region of higher velocity, hence the terminology convective part of \mathbf{a} .

Similarly, in cylindricals, the acceleration vector can be written as

$$\mathbf{a} = a_r \hat{\mathbf{e}}_r + a_\theta \hat{\mathbf{e}}_\theta + a_z \hat{\mathbf{e}}_z, \quad (7.23)$$

where it can be shown (Humphrey 2002) that the components are

$$\begin{aligned} a_r &= \frac{\partial v_r}{\partial t} + v_r \frac{\partial v_r}{\partial r} + \frac{v_\theta}{r} \frac{\partial v_r}{\partial \theta} - \frac{v_\theta^2}{r} + v_z \frac{\partial v_r}{\partial z}, \\ a_\theta &= \frac{\partial v_\theta}{\partial t} + v_r \frac{\partial v_\theta}{\partial r} + \frac{v_\theta}{r} \frac{\partial v_\theta}{\partial \theta} + \frac{v_r v_\theta}{r} + v_z \frac{\partial v_\theta}{\partial z}, \\ a_z &= \frac{\partial v_z}{\partial t} + v_r \frac{\partial v_z}{\partial r} + \frac{v_\theta}{r} \frac{\partial v_z}{\partial \theta} + v_z \frac{\partial v_z}{\partial z}. \end{aligned} \quad (7.24)$$

Note that “extra” terms arise in cylindrical coordinates [cf. Eq. (7.22)] because we are taking derivatives of the velocity (magnitude and direction) with respect to both time and direction. In contrast to Cartesian coordinates wherein $\partial(\hat{\mathbf{i}})/\partial x = \mathbf{0}$ and so forth, in cylindricals

$$\frac{\partial}{\partial \theta}(\hat{e}_r) = \hat{e}_\theta \quad \text{and} \quad \frac{\partial}{\partial \theta}(\hat{e}_\theta) = -\hat{e}_r, \quad (7.25)$$

as suggested by Fig. 7.3 and demonstrated in Appendix 7. These derivatives of the base vectors are very important to remember. Similarly, in spherical coordinates, acceleration becomes

$$\mathbf{a} = a_r \hat{e}_r + a_\theta \hat{e}_\theta + a_\phi \hat{e}_\phi, \quad (7.26)$$

for which it can be shown (Humphrey 2002) that

$$\begin{aligned} a_r &= \frac{\partial v_r}{\partial t} + v_r \frac{\partial v_r}{\partial r} + \frac{v_\theta}{r} \frac{\partial v_r}{\partial \theta} - \frac{v_\theta^2 + v_\phi^2}{r} + \frac{v_\phi}{r \sin \theta} \frac{\partial v_r}{\partial \phi}, \\ a_\theta &= \frac{\partial v_\theta}{\partial t} + v_r \frac{\partial v_\theta}{\partial r} + \frac{v_\theta}{r} \frac{\partial v_\theta}{\partial \theta} + \frac{v_r v_\theta}{r} - \frac{v_\phi^2}{r} \cot \theta + \frac{v_\phi}{r \sin \phi} \frac{\partial v_\theta}{\partial \phi}, \\ a_\phi &= \frac{\partial v_\phi}{\partial t} + v_r \frac{\partial v_\phi}{\partial r} + \frac{v_\theta}{r} \frac{\partial v_\phi}{\partial \theta} + \frac{v_r v_\phi}{r} + \frac{v_\theta v_\phi \cot \theta}{r} + \frac{v_\phi}{r \sin \phi} \frac{\partial v_\phi}{\partial \phi}. \end{aligned} \quad (7.27)$$

Again, the “extra” terms arise because of the derivatives of the base vectors, in particular

$$\begin{aligned} \frac{\partial}{\partial \theta}(\hat{e}_r) &= \hat{e}_\theta, & \frac{\partial}{\partial \theta}(\hat{e}_\theta) &= -\hat{e}_r, \\ \frac{\partial}{\partial \phi}(\hat{e}_r) &= \sin \theta \hat{e}_\phi, & \frac{\partial}{\partial \phi}(\hat{e}_\theta) &= \cos \theta \hat{e}_\phi, \end{aligned} \quad (7.28)$$

and

$$\frac{\partial}{\partial \phi}(\hat{e}_\phi) = -\sin \theta \hat{e}_r - \cos \theta \hat{e}_\theta. \quad (7.29)$$

We will use spherical coordinates in Chap. 11 to investigate the interaction of cerebrospinal fluid and an intracranial saccular aneurysm.

Example 7.1 Given the following velocity field, determine if the Eulerian acceleration is zero:

$$\mathbf{v} = Ax\hat{i} - Ay\hat{j},$$

where A is a number.

Solution: Although \mathbf{v} is independent of time and thus does not have a local component of acceleration (i.e., it is a steady flow), we must check the convective part. Note, therefore, that the Cartesian components of \mathbf{v} are

$$v_x = Ax, \quad v_y = -Ay$$

and the velocity gradients are

$$\frac{\partial v_x}{\partial x} = A, \quad \frac{\partial v_x}{\partial y} = 0, \quad \frac{\partial v_y}{\partial x} = 0, \quad \frac{\partial v_y}{\partial y} = -A.$$

Hence, from Eq. (7.22),

$$\mathbf{a} = [0 + Ax(A) + (-Ay)(0) + 0]\hat{\mathbf{i}} + [0 + Ax(0) + (-Ay)(-A) + 0]\hat{\mathbf{j}} + 0\hat{\mathbf{k}},$$

or

$$\mathbf{a} = A^2(x\hat{\mathbf{i}} + y\hat{\mathbf{j}})$$

and, consequently, the acceleration is not zero.

Before concluding this section, we emphasize that velocity and acceleration are both field quantities; that is, they depend on position as well as time in general. Consequently, it is useful to note some common terminology. A flow is said to be one, two, or three dimensional if the velocity field depends on, respectively, one, two, or three space variables. For example, with respect to Cartesians, a velocity field would be one dimensional if $\mathbf{v} = \mathbf{v}(x)$ but two dimensional if $\mathbf{v} = \mathbf{v}(x, y)$. Note, therefore, that one, two, or three dimensional does not have anything to do with the number of components, v_x , v_y , or v_z , that are nonzero; the dimensionality merely specifies the spatial dependence of all components. A flow in which only one component is nonzero with respect to a given coordinate system is said to be *unidirectional* regardless of its dependence on position.

Observation 7.1. Mathematically, a *field* is simply a contiguous collection of points in a region of space. When a quantity is defined at any such point, we say that it is a field quantity. Scalar quantities such as mass density, temperature, and pressure are examples of field quantities. Herein, we see too that velocity is

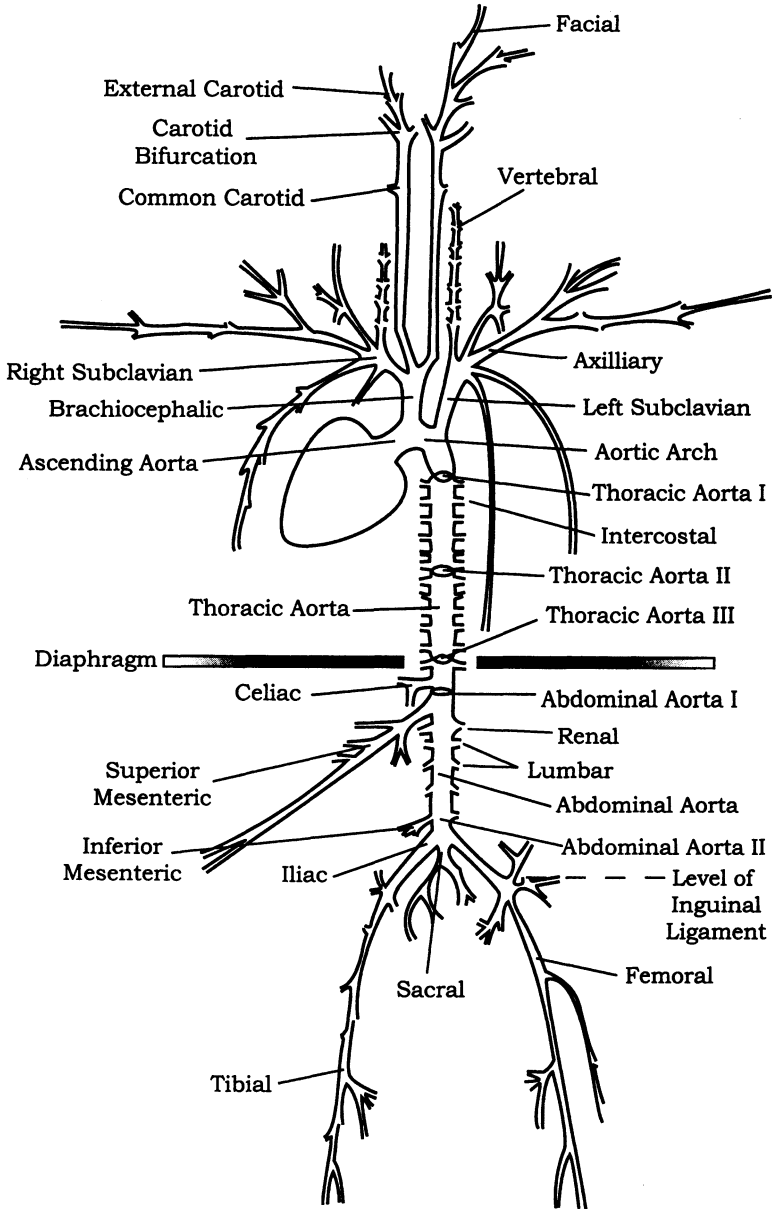


FIGURE 7.5 Schema of some of the large vessels that comprise the vasculature. There are, for example, $\sim 1.2 \times 10^5$ arteries, 2.8×10^6 arterioles, 2.7×10^9 capillaries, 1.0×10^7 venules, and 7.0×10^5 veins in a 20-kg dog. From Humphrey (2002), with permission.

a field quantity because it can depend on position as well as time. Figure 7.5 is a schematic drawing of part of the cardiovascular system of the dog. Clearly, the vasculature consists of a complex network of curved, tapering, and branching tubes called blood vessels. It is easy to imagine, therefore, that the velocity of the blood varies tremendously from point to point as well as throughout the cardiac cycle. Indeed, even locally within a curved region (aortic arch), bifurcation (aorto-iliac) or stenosis (Fig. 7.4), the velocity can vary tremendously in both magnitude and direction. The same is true, of course, in the airways within the lung and in the urinary tract. Quantification of the pressure and velocity fields is a prime objective in biofluid mechanics; this will require four governing equations, in general – one for pressure and one for each of the three components of velocity. We discuss these governing equations below.

7.3.2 Fluid Rotation

As noted above, we can imagine a fictitious cube of fluid (of mass Δm) rotating about all three axes x , y , and z . Such rotations can be described by an angular velocity vector, namely

$$\boldsymbol{\omega} = \omega_x \hat{\mathbf{i}} + \omega_y \hat{\mathbf{j}} + \omega_z \hat{\mathbf{k}}, \quad (7.30)$$

where ω_x is the rotation about the x axis, ω_y is the rotation about the y axis, and ω_z is the rotation about the z axis. To evaluate the components of this rotation vector $\boldsymbol{\omega}$, we may define the angular velocity about an axis as the average angular velocity of two initially perpendicular differential line segments in a plane perpendicular to the axis. For example, the component of rotation about the z axis is equal to the average angular velocity of two originally perpendicular infinitesimal line segments in the x - y plane (Fig. 7.6). The rate of rotation of line segment \overline{oa} of length Δx , is given by

$$\omega_{\theta a} = \lim_{\Delta t \rightarrow 0} \frac{\Delta \alpha}{\Delta t}, \quad (7.31)$$

where $\tan \Delta \alpha \sim \Delta \alpha$ for small-angle changes during the period Δt and $\tan \Delta \alpha$ is simply the opposite over the adjacent. (Note: In contrast to the small-angle assumption used by some to derive the small strain ϵ of Chap. 2, specification of a small-angle change here is not an assumption, it is merely consistent with the consideration of changes over a short interval of time Δt). If point o travels vertically at velocity v_y , then point a must have a greater velocity in order for $\Delta \alpha$ to change from 0 (at time $t = 0$) to some nonzero but small value at time $t + \Delta t$. Hence, if point a moves vertically at velocity $v_y + \Delta v_y$, then by the Taylor series expansion,

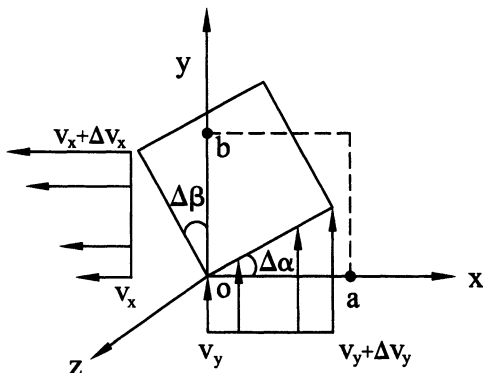


FIGURE 7.6 Rigid-body rotation of a fluid element in two dimensions. Note that such a rotation implies that the velocity must vary from point to point, such as the y -direction velocity at point a (e.g., $v_y + \Delta v_y$) must be greater than that at point o (e.g., v_y) for the line \overline{oa} to rotate counterclockwise. A similar difference must exist in v_x at points b and o .

$$\Delta v_y = \frac{\partial v_y}{\partial x} \Delta x + \text{H.O.T.} \tag{7.32}$$

where H.O.T. stands for higher-order terms, which are negligible with respect to terms that are linear in delta such as Δx or Δy (recall our derivation in Sect. 3.1). Thus, in the increment of time Δt , point a moves vertically a distance (which is given by a velocity multiplied by time)

$$\left(v_y + \frac{\partial v_y}{\partial x} \Delta x - v_y \right) \Delta t \tag{7.33}$$

relative to o , and ω_{oa} becomes

$$\omega_{oa} = \lim_{\Delta t \rightarrow 0} \frac{1}{\Delta t} \left(\frac{(\partial v_y / \partial x) \Delta x \Delta t}{\Delta x} \right) = \frac{\partial v_y}{\partial x}. \tag{7.34}$$

Similarly, the angular velocity of line segment \overline{ob} about the z axis is

$$\omega_{ob} = \lim_{\Delta t \rightarrow 0} \frac{\Delta \beta}{\Delta t}, \tag{7.35}$$

where b is moving in the negative x direction. If o moves leftward at velocity $-v_x$, then b must move at $-(v_x + \Delta v_x)$, where, again, we appeal to the Taylor's series. The distance along the negative x axis moved by b relative to o is thus

$$-\left(v_x + \frac{\partial v_x}{\partial y} \Delta y - v_x\right) \Delta t \quad (7.36)$$

and, therefore, ω_{ob} becomes

$$\omega_{ob} = \lim_{\Delta t \rightarrow 0} \frac{1}{\Delta t} \left(\frac{-(\partial v_x / \partial y) \Delta y \Delta t}{\Delta y} \right) = -\frac{\partial v_x}{\partial y}. \quad (7.37)$$

The mean angular velocity about the z axis, ω_z , is thus defined as the mean of ω_{oa} and ω_{ob} , or

$$\omega_z = \frac{1}{2} \left(\frac{\partial v_y}{\partial x} - \frac{\partial v_x}{\partial y} \right). \quad (7.38)$$

Similarly, for ω_x and ω_y , it is easy to show that (do it)

$$\omega_x = \frac{1}{2} \left(\frac{\partial v_z}{\partial y} - \frac{\partial v_y}{\partial z} \right), \omega_y = \frac{1}{2} \left(\frac{\partial v_x}{\partial z} - \frac{\partial v_z}{\partial x} \right), \quad (7.39)$$

where $\boldsymbol{\omega} = \omega_x \hat{\mathbf{i}} + \omega_y \hat{\mathbf{j}} + \omega_z \hat{\mathbf{k}}$, and therefore

$$\boldsymbol{\omega} = \frac{1}{2} \left[\left(\frac{\partial v_z}{\partial y} - \frac{\partial v_y}{\partial z} \right) \hat{\mathbf{i}} + \left(\frac{\partial v_x}{\partial z} - \frac{\partial v_z}{\partial x} \right) \hat{\mathbf{j}} + \left(\frac{\partial v_y}{\partial x} - \frac{\partial v_x}{\partial y} \right) \hat{\mathbf{k}} \right]. \quad (7.40)$$

If we recognize the term in the square brackets as the curl $\mathbf{v} \equiv \nabla \times \mathbf{v}$ in Cartesian coordinates, then we can rewrite this result in a more compact (and general) vector notation as

$$\boldsymbol{\omega} = \frac{1}{2} \nabla \times \mathbf{v}. \quad (7.41)$$

Moreover, if we define a new quantity, $\boldsymbol{\zeta} = 2\boldsymbol{\omega}$, then

$$\boldsymbol{\zeta} = \nabla \times \mathbf{v}, \quad (7.42)$$

where $\boldsymbol{\zeta}$ is called the *vorticity*—it is an alternate measure of the rotation of fluid elements. A flow in which the vorticity is zero is said to be *irrotational*. We will see later that irrotational flows allow significant simplification in the governing differential equations of motion; thus, it is useful to compute the vorticity for a given flow field.

Finally, note that in cylindrical coordinates, the vorticity is given by

$$\begin{aligned}\nabla \times \mathbf{v} = & \left(\frac{1}{r} \frac{\partial v_z}{\partial \theta} - \frac{\partial v_\theta}{\partial z} \right) \hat{\mathbf{e}}_r + \left(\frac{\partial v_r}{\partial z} - \frac{\partial v_z}{\partial r} \right) \hat{\mathbf{e}}_\theta \\ & + \left(\frac{1}{r} \frac{\partial (rv_\theta)}{\partial r} - \frac{1}{r} \frac{\partial v_r}{\partial \theta} \right) \hat{\mathbf{e}}_z.\end{aligned}\quad (7.43)$$

Likewise, in spherical coordinates, the vorticity is

$$\begin{aligned}\nabla \times \mathbf{v} = & \left(\frac{1}{r \sin \theta} \frac{\partial (v_\phi \sin \theta)}{\partial \theta} - \frac{1}{r \sin \theta} \frac{\partial v_\theta}{\partial \phi} \right) \hat{\mathbf{e}}_r \\ & + \left(\frac{1}{r \sin \theta} \frac{\partial v_r}{\partial \phi} - \frac{1}{r} \frac{\partial (rv_\phi)}{\partial r} \right) \hat{\mathbf{e}}_\theta + \left(\frac{1}{r} \frac{\partial (rv_\theta)}{\partial r} - \frac{1}{r} \frac{\partial v_r}{\partial \theta} \right) \hat{\mathbf{e}}_\phi.\end{aligned}\quad (7.44)$$

Here, we recognize one of the advantages of writing general results [Eq. (7.42)] in vector form. To derive Eqs. (7.43) and (7.44), we did not have to draw differential elements for cylindrical or spherical domains and determine how associated line elements rotate about each axis of interest; we merely used the del operator in the coordinate system of interest to compute general relations for the curl of the velocity. Such an approach is common in continuum mechanics: Based on the underlying physics, derive a relationship of interest with respect to Cartesian coordinates, which is generally the simplest to derive, and then extend the generalized result to other coordinate systems as needed using mathematical manipulations alone.

Example 7.2 Determine if the velocity field in Example 7.1 is irrotational.

Solution: Given that, $v_x = Ax$ and $v_y = -Ay$,

$$\boldsymbol{\zeta} = \frac{1}{2}(0 + 0)\hat{\mathbf{i}} + \frac{1}{2}(0 + 0)\hat{\mathbf{j}} + \frac{1}{2}(0 + 0)\hat{\mathbf{k}},$$

hence the velocity is irrotational.

7.3.3 Rate of Deformation

During extensional deformations, a fluid element will simply change in length. Rather than using strain to quantify the extension, as in solid mechanics, it proves to be convenient in fluid mechanics to focus on the rate of extension (i.e., the stretching or rate of strain). Like strain, such rates of change can also be described by nine scalar components relative to a coordinate system of interest,

six of which are independent. To measure the rate of change of extension in one direction, consider Fig. 7.4, in which a fluid accelerates, and thereby “stretches,” within a constriction. A normalized rate of extension (or stretching) can be defined as the rate at which a line element lengthens divided by its original length; that is, it can be computed by knowing the difference in lengths at two times. Let the original length be Δx at time t . For this length to have increased at time $t + \Delta t$, the various particles cannot have moved at the same velocity. Hence, let the leftmost points have velocity v_x and the rightmost points have velocity $v_x + \Delta v_x$, both at time $t + \Delta t$, which allows a lengthening. Because a distance can be computed via a velocity multiplied by time, we have the length $\Delta x + \Delta v_x \Delta t$ at time $t + \Delta t$. Hence, the rate of lengthening, normalized by the length at time t , is

$$D_{xx} = \lim_{\substack{\Delta t \rightarrow 0 \\ \Delta x \rightarrow 0}} \frac{1}{\Delta t} \left(\frac{(\Delta x + \Delta v_x \Delta t) - \Delta x}{\Delta x} \right), \quad (7.45)$$

where $\Delta v_x = (\partial v_x / \partial x) \Delta x$ from a Taylor’s series expansion: $v_x(x + \Delta x) = v_x(x) + (\partial v_x / \partial x) \Delta x + \text{H.O.T.}$ Thus, the rate of extension becomes

$$D_{xx} = \lim_{\substack{\Delta t \rightarrow 0 \\ \Delta x \rightarrow 0}} \frac{1}{\Delta t} \left(\frac{[\Delta x + (\partial v_x / \partial x) \Delta x \Delta t] - \Delta x}{\Delta x} \right) = \frac{\partial v_x}{\partial x}. \quad (7.46)$$

Likewise, it can be shown that

$$D_{yy} = \frac{\partial v_y}{\partial y}, D_{zz} = \frac{\partial v_z}{\partial z}. \quad (7.47)$$

Because they quantify rates at which lengths change, D_{xx} , D_{yy} , and D_{zz} are sometimes called components of a *stretching matrix* $[D]$. As an aside, it is interesting to note (do it) that

$$\nabla \cdot \mathbf{v} = \frac{\partial v_x}{\partial x} + \frac{\partial v_y}{\partial y} + \frac{\partial v_z}{\partial z} \equiv D_{xx} + D_{yy} + D_{zz}. \quad (7.48)$$

This will prove useful later. Indeed, a flow in which $\nabla \cdot \mathbf{v} = 0$ is said to be *incompressible* because it says that a fluid element that is lengthening in one direction must be thinning proportionately in other directions in order to conserve its volume.

Angular deformations of a fluid element involve changes in an angle between two initially perpendicular line segments in the fluid. To measure the rate of change of angles, or shear rates, consider the differential element in Fig. 7.7. In particular, imagine a rectangular fluid element that is contained between two

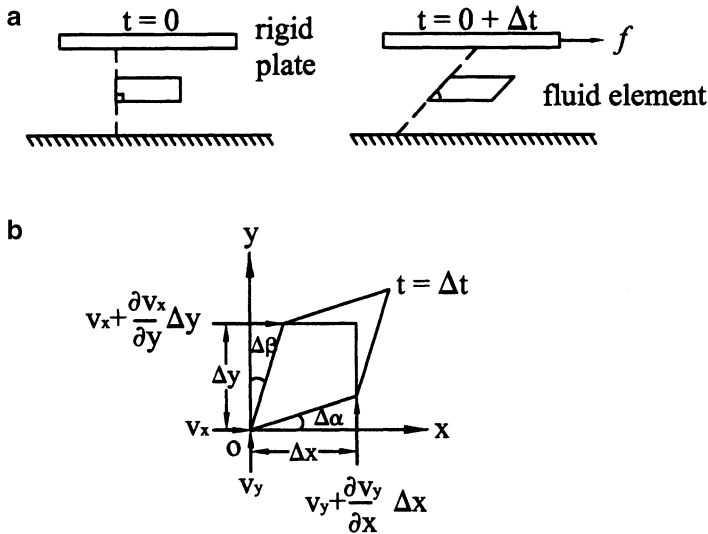


FIGURE 7.7 Panel (a): Schema of an experimental system that gives rise to a simple shear of a fluid element; panel (b): similar to Fig. 7.6 except for a pure shear rather than a rigid-body rotation. In this case, the internal angle decreases a small amount, $(\Delta\alpha + \Delta\beta)$, over an interval of time Δt .

solid plates and initially at rest. If the upper plate is moved with respect to a fixed lower plate, we can easily imagine that the fluid elements would be sheared (Fig. 7.7a). Similar to our analysis of the rigid rotation about the z axis [cf. Eq. (7.38)], let us consider the rate at which the internal angles change. For example (Fig. 7.7b), similar to Fig. 7.6

$$\tan \Delta\alpha = \frac{\{[v_y + (\partial v_y / \partial x) \Delta x] - v_y\} \Delta t}{\Delta x}, \tag{7.49}$$

whereas in contrast to Fig. 7.6,

$$\tan \Delta\beta = \frac{\{[v_x + (\partial v_x / \partial y) \Delta y] - v_x\} \Delta t}{\Delta y}, \tag{7.50}$$

because the enclosed angle is assumed to get smaller over time during a (positive) shearing motion (i.e., we are not looking at rigid-body rotation as before). Because these results are good for a short interval of time Δt , note that $\Delta\alpha$ and $\Delta\beta$ must likewise be small. By the small-angle approximation, therefore, $\tan \Delta\alpha \cong \Delta\alpha$ and $\tan \Delta\beta \cong \Delta\beta$ and we have

$$\begin{aligned}\Delta\alpha &\approx \frac{\{[v_y + (\partial v_y/\partial x)\Delta x] - v_y\}\Delta t}{\Delta x}, \\ \Delta\beta &\approx \frac{\{[v_x + (\partial v_x/\partial y)\Delta y] - v_x\}\Delta t}{\Delta y}.\end{aligned}\quad (7.51)$$

To find the rate at which these angles change, take the limit as $\Delta t \rightarrow 0$ of the time-averaged mean of the two changes in angle, namely

$$D_{xy} = \lim_{\Delta t \rightarrow 0} \frac{1}{\Delta t} \left(\lim_{\substack{\Delta x \rightarrow 0 \\ \Delta y \rightarrow 0}} \frac{1}{2} (\Delta\alpha + \Delta\beta) \right) = \lim_{\Delta t \rightarrow 0} \frac{1}{\Delta t} \left[\frac{1}{2} \left(\frac{\partial v_y}{\partial x} \Delta t + \frac{\partial v_x}{\partial y} \Delta t \right) \right], \quad (7.52)$$

or

$$D_{xy} = \frac{1}{2} \left(\frac{\partial v_y}{\partial x} + \frac{\partial v_x}{\partial y} \right). \quad (7.53)$$

It is easy to show (do it) that

$$D_{xz} = \frac{1}{2} \left(\frac{\partial v_x}{\partial z} + \frac{\partial v_z}{\partial x} \right), \quad D_{yz} = \frac{1}{2} \left(\frac{\partial v_y}{\partial z} + \frac{\partial v_z}{\partial y} \right). \quad (7.54)$$

Similar to the situation for strains, which are useful measures of the deformation in solids, it can be shown that, by definition, $D_{xy} = D_{yx}$, $D_{xz} = D_{zx}$ and $D_{yz} = D_{zy}$. These quantities can thus be written in (a symmetric) matrix form as follows:

$$[D] = \begin{bmatrix} D_{xx} & D_{xy} & D_{xz} \\ D_{yx} & D_{yy} & D_{yz} \\ D_{zx} & D_{zy} & D_{zz} \end{bmatrix}, \quad (7.55)$$

where

$$\begin{aligned}D_{xx} &= \frac{\partial v_x}{\partial x}, & D_{xy} &= \frac{1}{2} \left(\frac{\partial v_y}{\partial x} + \frac{\partial v_x}{\partial y} \right) = D_{yx}, \\ D_{yy} &= \frac{\partial v_y}{\partial y}, & D_{yz} &= \frac{1}{2} \left(\frac{\partial v_y}{\partial z} + \frac{\partial v_z}{\partial y} \right) = D_{zy}, \\ D_{zz} &= \frac{\partial v_z}{\partial z}, & D_{zx} &= \frac{1}{2} \left(\frac{\partial v_x}{\partial z} + \frac{\partial v_z}{\partial x} \right) = D_{xz}.\end{aligned}\quad (7.56)$$

Similarly, it can be shown that in cylindrical,

$$[D] = \begin{bmatrix} D_{rr} & D_{r\theta} & D_{rz} \\ D_{\theta r} & D_{\theta\theta} & D_{\theta z} \\ D_{zr} & D_{z\theta} & D_{zz} \end{bmatrix}, \quad (7.57)$$

where

$$\begin{aligned} D_{rr} &= \frac{\partial v_r}{\partial r}, & D_{r\theta} &= \frac{1}{2} \left(r \frac{\partial}{\partial r} \left(\frac{v_\theta}{r} \right) + \frac{1}{r} \frac{\partial v_r}{\partial \theta} \right) = D_{\theta r}, \\ D_{\theta\theta} &= \frac{1}{r} \frac{\partial v_\theta}{\partial \theta} + \frac{v_r}{r}, & D_{\theta z} &= \frac{1}{2} \left(\frac{1}{r} \frac{\partial v_z}{\partial \theta} + \frac{\partial v_\theta}{\partial z} \right) = D_{z\theta}, \\ D_{zz} &= \frac{\partial v_z}{\partial z}, & D_{zr} &= \frac{1}{2} \left(\frac{\partial v_r}{\partial z} + \frac{\partial v_z}{\partial r} \right) = D_{rz}. \end{aligned} \quad (7.58)$$

Finally, in spherical coordinates, it can be shown that

$$[D] = \begin{bmatrix} D_{rr} & D_{r\theta} & D_{r\phi} \\ D_{\theta r} & D_{\theta\theta} & D_{\theta\phi} \\ D_{\phi r} & D_{\phi\theta} & D_{\phi\phi} \end{bmatrix}, \quad (7.59)$$

where

$$\begin{aligned} D_{rr} &= \frac{\partial v_r}{\partial r}, & D_{r\theta} &= \frac{1}{2} \left(r \frac{\partial}{\partial r} \left(\frac{v_\theta}{r} \right) + \frac{1}{r} \frac{\partial v_r}{\partial \theta} \right) = D_{\theta r}, \\ D_{\theta\theta} &= \frac{1}{r} \frac{\partial v_\theta}{\partial \theta} + \frac{v_r}{r}, & D_{\theta\phi} &= \frac{1}{2} \left(\frac{\sin \theta}{r} \frac{\partial}{\partial \theta} \left(\frac{v_\phi}{\sin \theta} \right) + \frac{1}{r \sin \theta} \frac{\partial v_\theta}{\partial \phi} \right) = D_{\phi\theta}, \\ D_{\phi\phi} &= \frac{1}{r \sin \theta} \frac{\partial v_\phi}{\partial \phi} + \frac{v_r}{r} + \frac{v_\theta \cot \theta}{r}, \\ D_{r\phi} &= \frac{1}{2} \left(\frac{1}{r \sin \theta} \frac{\partial v_r}{\partial \phi} + r \frac{\partial}{\partial r} \left(\frac{v_\phi}{r} \right) \right) = D_{\phi r}. \end{aligned} \quad (7.60)$$

Here, let us make a few observations. First, recall from Chap. 2 that although displacements \mathbf{u} are intuitive and measured easily, it was discovered that particular combinations of *displacement gradients* (called strains) are more useful in the analysis of the mechanics of solids. So, too, in fluid mechanics, we will see that combinations of *velocity gradients* are more useful in analysis than the intuitive and easily measured velocities \mathbf{v} . This reminds us that theory and its associated concepts, not simply the ease of making a measurement, must guide experimentation. Second, whereas the diagonal terms of $[D]$ provide information on rates of change of lengths, or stretching, the off-diagonal terms provide information on rates of change of internal angles, or shearing. Because of this, some prefer to refer to $[D]$ as a rate of deformation rather than a measure of stretching; indeed, others refer to it as a strain rate, for it is easily

seen that the components of $[D]$ could be computed from the components of the strain $[\varepsilon]$ if the displacement gradients were computed with respect to the original not current positions (i.e., with respect to \mathbf{X} not \mathbf{x}). Because $[\varepsilon]$ is based on a linearization of the exact measure of strain $[E]$, however, this correspondence may lead one to the false conclusion that $[D]$ is also a linearization of some measure of the motion—it is not. The small changes in lengths and angles used in deriving the components of $[D]$ are consistent with the small time steps $\Delta t \rightarrow 0$; hence, there is no linearization. The take-home message, therefore, is that regardless of its name (stretching, rate of deformation, or strain rate), $[D]$ is an exact, useful measure of the motion of particles in a fluid, just as $[E]$ is an exact, useful measure of the motion of particles in a solid. That said, we shall refer to $[D]$ as a *rate of deformation* and the particular off-diagonal terms as *shear rates*.

Example 7.3 Compute the components of $[D]$ for the velocity field in Example 7.1. Consider only x - y terms.

Solution: Given that $\mathbf{v} = Ax\hat{\mathbf{i}} - Ay\hat{\mathbf{j}}$ we have

$$\begin{aligned} D_{xx} &= \frac{\partial v_x}{\partial x} = A, & D_{xy} &= \frac{1}{2} \left(\frac{\partial v_y}{\partial x} + \frac{\partial v_x}{\partial y} \right) = 0, \\ D_{yx} &= \frac{1}{2} \left(\frac{\partial v_y}{\partial x} + \frac{\partial v_x}{\partial y} \right) = 0, & D_{yy} &= \frac{\partial v_y}{\partial y} = -A. \end{aligned}$$

Relative to x and y , therefore, we would say that this flow is shearless as well as irrotational (see Example 7.2).

Example 7.4 Determine the divergence of the velocity field in Example 7.3.

Solution:

$$\nabla \cdot \mathbf{v} = \frac{\partial v_x}{\partial x} + \frac{\partial v_y}{\partial y} + \frac{\partial v_z}{\partial z} = A + (-A) + 0 = 0.$$

Hence, based on the above definition, this flow is incompressible (i.e., volume conserving).

Again, that $\nabla \cdot \mathbf{v} = 0$ implies conservation of mass for an incompressible fluid will be proven in Sect. 8.1 of Chap. 8.

7.4 Constitutive Behavior

Recall from Chap. 2 that a constitutive relation describes the response of a material to applied loads under conditions of interest, which, of course, depends on the internal constitution of the material. Thus, metals behave differently than

polymers, and so too water behaves differently than glycerin, which behaves differently than blood, and so on. Recall, too, that in biosolid mechanics, we sought to relate stress to strain to describe linear and nonlinear elastic behaviors (Chaps. 2 and 6). In contrast, experience has proven that it is more useful to relate stress to rates of deformation in order to describe the behavior of most fluids. Nevertheless, as is the case for solids, the formulation of a constitutive relation for a fluid involves five steps (DEICE): delineating general characteristics, establishing an appropriate theoretical framework, identifying a specific form of the relation, calculating best-fit values of the material parameters, and evaluating the predictive capability of the final relation. Let us now consider in detail one class of fluids that we will focus on herein.

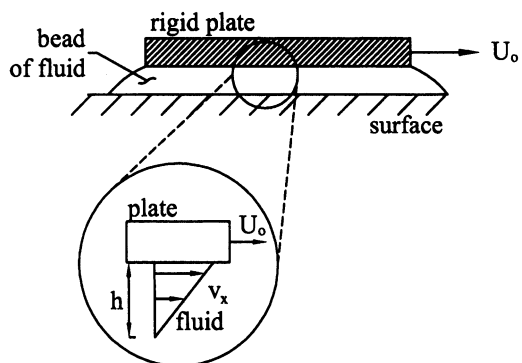
7.4.1 Newtonian Behavior

To begin our discussion of the experimental investigation of the constitutive behavior of fluids, let us consider a greatly simplified situation. Assume that we can pour a fluid onto a flat surface such that it does not wet the surface (i.e., it forms a broad “bead” of fluid like water on a newly waxed car). Moreover, assume that we can place a thin rigid solid plate on this thin layer of fluid, giving a situation like that in Fig. 7.8. Let us then apply an end load to the plate, which causes it to move at a constant velocity U_0 in the x direction, which, in turn, causes the fluid to flow. If *the fluid has the same velocity, at the points of contact, as the solid that it contacts*, and ignoring effects near the ends (e.g., surface tension), the velocity field \mathbf{v} in this simple case is $\mathbf{v} = v_x(y)\hat{\mathbf{i}}$, where

$$v_x = U_0 \left(\frac{y}{h} \right), v_y = 0, v_z = 0. \quad (7.61)$$

In particular, note that $v_x(y=0) = 0$ and $v_x(y=h) = U_0$, the velocities of the bottom surface and the top plate, respectively. Assuming that a fluid has the

FIGURE 7.8 Couette flow between two rigid parallel plates. The bottom plate is stationary, whereas the top plate moves at velocity U_0 in the positive x direction.



same velocity as the solid it contacts is called the *no-slip boundary condition*. Albeit an approximation, this assumption tends to be very good in many cases.

Consequently, the only nonzero component of $[D]$, from Eq. (7.56), is

$$D_{xy} = \frac{1}{2} \left(\frac{\partial v_y}{\partial x} + \frac{\partial v_x}{\partial y} \right) = \frac{1}{2} \left(0 + \frac{U_0}{h} \right) = D_{yx}, \quad (7.62)$$

which we note is the same at all points (x, y, z) in the fluid (if we are away from the end effects). By definition, the shear stress σ_{xy} exerted on the fluid by the plate is equal and opposite the shear stress imposed by the fluid on the plate (by Newton's third law). In this case, $\sigma_{yx} = f/A$, where f is the applied load and A is the surface area of contact between the plate and fluid. It is observed experimentally that the fluid shear stress σ_{yx} is related linearly to its shear rate D_{yx} for many fluids under many conditions (Fig. 7.9). Convention dictates that the slope of this shear stress versus shear-rate relation be denoted as 2μ , where μ is the (absolute) viscosity, much like the shear modulus G for solids. Viscosity is thus an important property of many fluids. Simply put, *viscosity* is a measure of the resistance to flow when a fluid is acted upon by a shear stress; in other words, it is a measure of the "thickness" of the fluid. Molasses, for example, is much more viscous than water (at the same temperature).

In most fluids, repeating this simple experiment in the y and z directions will result in the same slope 2μ (i.e., the same linear relationship between σ_{yz} and D_{yz} and σ_{xz} and D_{xz}). Hence, the response of many fluids is typically isotropic (i.e., independent of direction). Common experience reveals further that a fluid can also support a pressure p and that if compressible, experiments reveal that the normal stress will vary linearly with $\nabla \cdot \mathbf{v}$, a measure of the volume change.

When a fluid exhibits these linear and isotropic characteristics, it is said to be *Newtonian* to commemorate Sir I. Newton's (1642–1727) suggestion that the

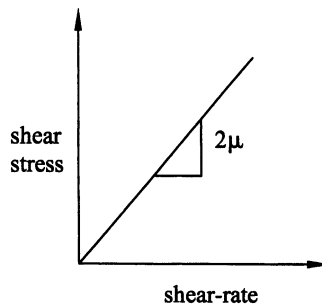


FIGURE 7.9 Shear stress plotted versus shear rate for a Newtonian fluid. Note the linear relationship, the slope of which is denoted by 2μ , where μ is the (absolute) viscosity. The factor 2 is included simply to cancel the $1/2$ that appears in the expression for shear rates [e.g., D_{xy} , as in Eq. (7.56)].

shear response of fluids was proportional to the shearing force. Newton did not formulate his mechanics for continua, however, nor did he have the concepts of stress, strain, or shear rates. As noted in Chap. 2, these ideas came later, due largely to L. Euler (1707–1783) and A. Cauchy (1789–1857). Hence, formal quantification of this linear behavior of fluids, based on extensive experimentation, was put in mathematical form much later and is given by the Navier–Poisson equations⁴

$$\begin{aligned}\sigma_{xx} &= -p + \lambda(\nabla \cdot \mathbf{v}) + 2\mu D_{xx}, & \sigma_{xy} &= 2\mu D_{xy} = \sigma_{yx}, \\ \sigma_{yy} &= -p + \lambda(\nabla \cdot \mathbf{v}) + 2\mu D_{yy}, & \sigma_{yz} &= 2\mu D_{yz} = \sigma_{zy}, \\ \sigma_{zz} &= -p + \lambda(\nabla \cdot \mathbf{v}) + 2\mu D_{zz}, & \sigma_{xz} &= 2\mu D_{xz} = \sigma_{zx}.\end{aligned}\quad (7.63)$$

where $\nabla \cdot \mathbf{v} = D_{xx} + D_{yy} + D_{zz}$ [Eq. (7.48)] and λ is a second material property/parameter. G. Stokes (1819–1903) hypothesized that $\lambda \sim -2\mu/3$, which is often employed. Regardless, these Navier–Poisson equations are similar for other coordinate systems, such as for cylindricals,

$$\begin{aligned}\sigma_{rr} &= -p + \lambda(\nabla \cdot \mathbf{v}) + 2\mu D_{rr}, & \sigma_{r\theta} &= 2\mu D_{r\theta} = \sigma_{\theta r}, \\ \sigma_{\theta\theta} &= -p + \lambda(\nabla \cdot \mathbf{v}) + 2\mu D_{\theta\theta}, & \sigma_{\theta z} &= 2\mu D_{\theta z} = \sigma_{z\theta}, \\ \sigma_{zz} &= -p + \lambda(\nabla \cdot \mathbf{v}) + 2\mu D_{zz}, & \sigma_{rz} &= 2\mu D_{rz} = \sigma_{zr}.\end{aligned}\quad (7.64)$$

and sphericals,

$$\begin{aligned}\sigma_{rr} &= -p + \lambda(\nabla \cdot \mathbf{v}) + 2\mu D_{rr}, & \sigma_{r\theta} &= 2\mu D_{r\theta} = \sigma_{\theta r}, \\ \sigma_{\theta\theta} &= -p + \lambda(\nabla \cdot \mathbf{v}) + 2\mu D_{\theta\theta}, & \sigma_{r\phi} &= 2\mu D_{r\phi} = \sigma_{\phi r}, \\ \sigma_{\phi\phi} &= -p + \lambda(\nabla \cdot \mathbf{v}) + 2\mu D_{\phi\phi}, & \sigma_{\theta\phi} &= 2\mu D_{\theta\phi} = \sigma_{\phi\theta}.\end{aligned}\quad (7.65)$$

In the case of an incompressible behavior, it can be shown (see Chap. 8) that $\nabla \cdot \mathbf{v} = 0$ and thus the Stoke’s hypothesis for λ becomes a moot point. Of course, when $\nabla \cdot \mathbf{v} = 0$, these constitutive equations simplify tremendously. For example, for an incompressible, Newtonian behavior, relative to Cartesian coordinates, we have the *incompressible Navier–Poisson equations* [recalling Eq. (7.56)]

$$\begin{aligned}\sigma_{xx} &= -p + 2\mu \frac{\partial v_x}{\partial x}, & \sigma_{xy} &= \mu \left(\frac{\partial v_y}{\partial x} + \frac{\partial v_x}{\partial y} \right) = \sigma_{yx}, \\ \sigma_{yy} &= -p + 2\mu \frac{\partial v_y}{\partial y}, & \sigma_{xz} &= \mu \left(\frac{\partial v_x}{\partial z} + \frac{\partial v_z}{\partial x} \right) = \sigma_{zx}, \\ \sigma_{zz} &= -p + 2\mu \frac{\partial v_z}{\partial z}, & \sigma_{yz} &= \mu \left(\frac{\partial v_y}{\partial z} + \frac{\partial v_z}{\partial y} \right) = \sigma_{zy},\end{aligned}\quad (7.66)$$

⁴ L. Navier (1785–1836) and S. D. Poisson (1781–1840).

which we shall use extensively in Chaps. 8 and 9; they are directly analogous to the so-called Hooke's law for solids [Exercise 2.18], which relates the stresses and strains in a linear fashion.⁵ Indeed, Hooke's law was also formulated by Navier and others in the nineteenth century; it contains two independent material parameters in the case of isotropy (E and ν), similar to the compressible Navier–Poisson equation (with parameters μ and λ). As noted earlier, however, pressure plays a particularly important role in the constitutive relation here in contrast to that for a Hookean solid.

Example 7.5 Although the p that appears in Eq. (7.66) is actually a Lagrange multiplier that enforces the incompressibility constraint, similar to its role in Eq. (6.76) for nonlinear solids, its value is equivalent to the hydrostatic pressure for an incompressible Newtonian fluid. Prove this.

Solution: Recall from Eq. (7.3) that the hydrostatic pressure is defined as

$$p = -\frac{1}{3}(\sigma_{xx} + \sigma_{yy} + \sigma_{zz});$$

hence, for the incompressible Navier–Poisson relation, we have

$$\begin{aligned} -\frac{1}{3}(\sigma_{xx} + \sigma_{yy} + \sigma_{zz}) &= -\frac{1}{3}(-p + 2\mu D_{xx} - p + 2\mu D_{yy} - p + 2\mu D_{zz}) \\ &= p - \frac{2}{3}\mu(D_{xx} + D_{yy} + D_{zz}) \\ &= p - \frac{2}{3}\mu\left(\frac{\partial v_x}{\partial x} + \frac{\partial v_y}{\partial y} + \frac{\partial v_z}{\partial z}\right) \\ &= p - \frac{2}{3}\mu(\nabla \cdot \mathbf{v}), \end{aligned}$$

where we said that $\nabla \cdot \mathbf{v}$ will be shown to be zero for incompressible flows. In this case, therefore, the p in Eq. (7.66) is the hydrostatic pressure. This is not true, in general, for incompressible solids. Finally, note the term $-\frac{2}{3}\mu$ that multiplies the divergence of the velocity. This term reveals where the aforementioned Stokes' hypothesis originated.

⁵ It is interesting that the simple (i.e., linear) descriptions of solid and fluid behavior are called Hookean and Newtonian after the contemporaries/adversaries R. Hooke and Sir I. Newton even though the particular equations were put forth much later.

Example 7.6 In the case of pure *fluid statics*, the fluid is at rest and thus the velocity and acceleration of the fluid are both zero (note: actually, we only need $\mathbf{a} = \mathbf{0}$ for statics by Newton's second law). Show that in this case, the only possible stress in the fluid is a hydrostatic pressure. Moreover, show that if a cube of a static fluid is oriented with respect to an $(o; x, y, z)$ coordinate system, then the only stresses with respect to an $(o; x', y', z')$ coordinate system are still hydrostatic.

Solution: If $\mathbf{v} = \mathbf{0}$, then $v_x = v_y = v_z = 0$ and all components of $[D]$ are zero. From Eq. (7.66), therefore,

$$\begin{aligned}\sigma_{xx} &= -p, & \sigma_{yy} &= -p, & \sigma_{zz} &= -p, \\ \sigma_{xy} &= 0 = \sigma_{yx}, & \sigma_{xz} &= 0 = \sigma_{zx}, & \sigma_{yz} &= 0 = \sigma_{zy}\end{aligned}$$

and the stress is *hydrostatic* (i.e., the normal stresses at a point equal the negative of the pressure at that point). Moreover, if we consider a rotation about the z axis (i.e., in the x - y plane), then

$$\begin{aligned}\sigma'_{xx} &= \sigma_{xx} \cos^2 \alpha + 2\sigma_{xy} \cos \alpha \sin \alpha + \sigma_{yy} \sin^2 \alpha, \\ \sigma'_{xy} &= (\sigma_{yy} - \sigma_{xx}) \cos \alpha \sin \alpha + \sigma_{xy} (\cos^2 \alpha - \sin^2 \alpha), \\ \sigma'_{yy} &= \sigma_{xx} \sin^2 \alpha - 2\sigma_{xy} \cos \alpha \sin \alpha + \sigma_{yy} \cos^2 \alpha\end{aligned}$$

from Eqs. (2.13), (2.17), and (2.21). Hence, in our case,

$$\begin{aligned}\sigma'_{xx} &= -p \cos^2 \alpha + 0 - p \sin^2 \alpha = -p, \\ \sigma'_{xy} &= (-p + p) \cos \alpha \sin \alpha + 0 = 0, \\ \sigma'_{yy} &= -p \sin^2 \alpha - 0 - p \cos^2 \alpha = -p\end{aligned}$$

for all α , and the stress is indeed hydrostatic in pure fluid statics regardless of the coordinate system (Fig. 7.10).

Although discussed in detail in Chap. 8, note that if μ is negligible, then

$$\sigma_{xx} = -p, \quad \sigma_{yy} = -p, \quad \sigma_{zz} = -p \quad (7.67)$$

and all shear stresses are zero. A fluid that can only support a pressure, not a shear stress, is said to be *inviscid*. Whereas no fluid has zero viscosity, the assumption of negligible viscosity (like that of a rigid member in a truss in statics even though no material is truly rigid) has proven useful in many areas of fluid mechanics, particularly in aerospace applications.

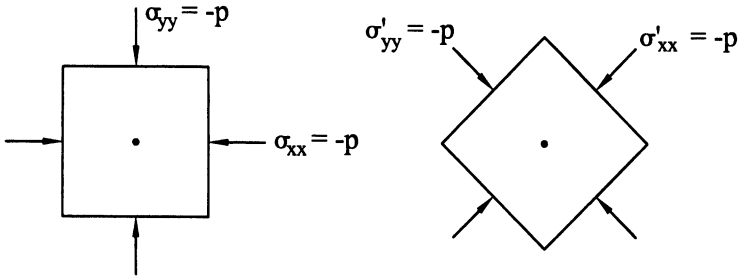


FIGURE 7.10 So-called hydrostatic state of stress (shown in two dimensions simply for convenience) wherein the normal components each equal $-p$, the fluid pressure, and the shear components are all zero—both relative to all coordinate systems.

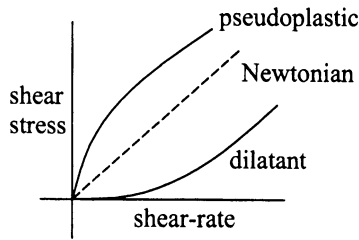


FIGURE 7.11 Two common non-Newtonian (i.e., nonlinear) behaviors exhibited by fluids. A pseudoplastic behavior is characterized by a resistance to flow that decreases with increasing shear rates, whereas a dilatant behavior is characterized by a resistance to flow that increases with increasing shear rates. In both cases, the behavior at high shear rates appears Newtonian; that is, the resistance to flow (or viscosity) is nearly constant at high shear rates. Note, too, that the pseudoplastic and dilatant behaviors are illustrative only; they could appear on either side of the Newtonian curve, the slope of which varies from fluid to fluid and with temperature.

7.4.2 Non-Newtonian Behavior

Not all fluids exhibit a Newtonian (i.e., linear) behavior. Figure 7.11 contrasts a Newtonian behavior with two general non-Newtonian behaviors: pseudoplastic and dilatant. *Pseudoplastic behavior* is characterized by a viscosity (i.e., resistance to flow) that is lower at higher shear rates than it is at lower shear rates; for this reason, pseudoplastic behavior is sometimes called *shear thinning*. This can be due to particles within the fluid that aggregate at low shear rates but “break up” at higher shear rates, which lowers the viscosity. Of particular importance in biofluids, whole blood is such a fluid. At low shear rates, the red blood cells tend to aggregate, a phenomenon known as *rouleaux* (Fig. 7.12), which depends on the presence of fibrinogen and the globulins. Of course, in the limit as the shear rate goes to zero, the blood will tend to aggregate further, eventually

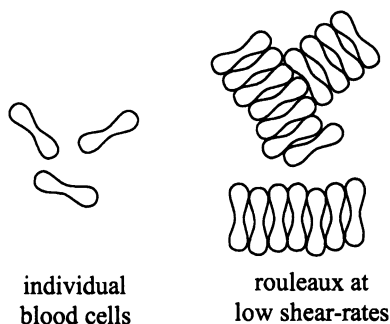


FIGURE 7.12 Aggregation of red blood cells, called rouleaux, that occurs at low shear rates. Such aggregation tends to increase the resistance of blood to flow at low shear rates and thus is responsible in part for the pseudoplastic type of behavior of blood.

leading to a process known as clotting, which involves additional mechanisms, including platelet activation and the conversion of fibrinogen to fibrin, an essential component of a clot. As the shear rate increases from low, but nonzero values, however, the rouleaux break up and blood behaves like a Newtonian fluid; the latter is often assumed in large arteries, thus, $\mu \sim \text{constant}$ (often cited to be ~ 3.5 cP, or centiPoise) and one can employ the Navier–Poisson equations to describe many flows of blood in large arteries. Plasma (i.e., whole blood minus cells) always behaves as a Newtonian fluid, with a viscosity $\mu \sim 1.2$ cP. It should also be noted, however, that in capillaries, which are $\sim 5\text{--}8$ μm in diameter, the red blood cells go through one at a time, with plasma in between. In this case, the blood should be treated as a two-phase flow—a solid and fluid mixture, which is beyond the scope of this book.

Because of its non-Newtonian behavior, whole blood has been modeled using various relations.⁶ For example, Fung (1990) advocates the following model for blood:

$$\begin{aligned} \sigma_{xx} &= -p + 2\eta(J_2)D_{xx}, & \sigma_{xy} &= 2\eta(J_2)D_{xy}, \\ \sigma_{yy} &= -p + 2\eta(J_2)D_{yy}, & \sigma_{yz} &= 2\eta(J_2)D_{yz}, \\ \sigma_{zz} &= -p + 2\eta(J_2)D_{zz}, & \sigma_{xz} &= 2\eta(J_2)D_{xz}, \end{aligned} \quad (7.68)$$

where

$$\eta(J_2) = \frac{1}{\sqrt{J_2}} \left((\mu^2 J_2)^{1/4} + \frac{1}{\sqrt{2}} \sqrt{\tau_y} \right)^2, \quad (7.69)$$

⁶ When behavior is linear, the relation is unique; when the behavior is nonlinear, many different constitutive relations can often “fit” the data.

$$J_2 = \frac{1}{2}(D_{xx} + D_{yy} + D_{zz} + 2D_{xy}D_{yx} + 2D_{xz}D_{zx} + 2D_{yz}D_{zy}), \quad (7.70)$$

and μ is a viscosity at a high shear rate and τ_y is a solidlike yield stress at low shear rates. To better appreciate the implications of this complex relation, let us return to the simple experiment in Fig. 7.8, which allowed our observation of linear behavior for a Newtonian fluid. In this simple case, D_{xy} is nonzero and all other components of $[D]$ are zero. Hence, Fung's relation reduces to

$$\sigma_{xy} = 2\eta(J_2)D_{xy}, \quad (7.71)$$

with

$$\eta(J_2) = \frac{1}{\sqrt{D_{xy}^2}} \left((\mu^2 D_{xy}^2)^{1/4} + \frac{1}{\sqrt{2}} \sqrt{\tau_y} \right)^2. \quad (7.72)$$

When D_{xy} is very small, η tends to become large, its value depending largely on the values of $\tau_y/2D_{xy}$; τ_y is also small, usually on the order of 0.005 Pa. Conversely, when D_{xy} is large, the yield stress becomes negligible and $\eta \cong \mu$, the Newtonian case wherein $\sigma_{xy} = 2\mu D_{xy}$. Hence, Fung's relation accounts for the pseudoplastic character illustrated in Fig. 7.11, including Newtonian behavior at high shear rates.

Because the pseudoplastic character of blood is due largely to the red blood cells, note the following. At a low hematocrit H (i.e., percent concentration of red blood cells), such as $H \sim 8.25\%$, $\eta(J_2)$ is nearly constant (i.e., $\eta \sim \mu$) over a range of shear rates from 0.1 to 1,000 s^{-1} . For $H \sim 18\%$, however, $\eta(J_2)$ is nearly constant only for shear rates above 600 s^{-1} . Normal shear rates range from 100 to 2,000 s^{-1} in large arteries and from 20 to 200 s^{-1} in large to small veins. Normal values of the hematocrit are about 42 and 47 % in women and men, respectively, hence the Newtonian response only at high shear rates. As noted earlier, the value of $\eta(J_2)$ at high shear rates is on the order of 2–3.5 cP for whole blood. Note: 1 Poise = 0.1 kg/ms = 0.1 Ns/m², where cP denotes centiPoise (after J. Poiseuille).

A good example of a *dilatant behavior* is given by a cornstarch solution. As some learn in kindergarten, slowly pulling one's fingers through a cornstarch solution meets little resistance, whereas quickly pulling one's fingers meets with considerable resistance; that is, the apparent viscosity increases with increased shear rate (cf. Fig. 7.11). Dilatant behavior is typical of suspension of solids, in which the solid content is very high (e.g., 80 %) so that it forms large masses within the suspension. Increasing shear rates break up such masses.

Finally, note that some fluids exhibit a changing (apparent) viscosity over time when at a constant shear rate; that is, an internal structure may build up or break down over time. A non-Newtonian behavior characterized by a decreasing viscosity over time is called *thixotropic*; one characterized by an increasing viscosity over time of shear is called *rheopectic*. Because of these behaviors, a hysteresis loop will be seen in plots of shear stress versus shear rate if the fluid is sheared at an increasing rate for some time followed by a decreasing rate. Some man-made models of synovial fluid exhibit such non-Newtonian characteristics. Synovial fluid is found in articulating joints and is a remarkable lubricant. It shall be discussed in more detail later.

Observation 7.2. We discuss in Chap. 11 multiple examples wherein one must study together the fluid and the solid mechanics; such problems are often referred to as *fluid-solid interaction* (FSI) problems. One of the most important interactions in the vasculature is the cyclic deformation of the arterial wall in response to local changes in blood pressure that occur throughout the cardiac cycle; such deformations change the domain through which the blood flows and hence the hemodynamics. One of the earliest studies of such fluid-solid interactions resulted in the so-called Moens-Korteweg equation, which can be written $c^2 = Eh/2\rho a$, where c is the speed of the pressure wave, E is the Young's modulus of linearized isotropic elasticity, h and a are the thickness and inner radius of the tube, respectively, and ρ is the mass density of the fluid (see Example 11.1). Hence, the wave speed c depends on both the geometry (a and h) and physical properties (E and ρ), noting that Eh reveals that it is the structural (not just material) stiffness that governs the pressure wave. As expected, this equation predicts that the wave speed becomes infinite when E becomes infinite, that is, if the tube is rigid. This observation warns us of inherent limitations of solutions of the Navier–Stokes equations such as those presented in Sects. 9.2, 9.4, and 9.5, each of which assumes a rigid wall.

The fundamental importance of pulse wave velocity in central arteries (e.g., the aorta and carotid arteries) has been recognized over the past few decades. For example, an increased pulse wave velocity within the aorta causes the reflected waves to return earlier during the cardiac cycle, thus augmenting the systolic blood pressure in the proximal aorta rather than the diastolic pressure, as in health. Increased systolic pressure and decreased diastolic pressure in the proximal aorta results in an increased workload on the heart and decreased coronary perfusion during diastole, both of which decrease cardiac function. Although the Moens-Korteweg equation does not strictly apply to the arterial tree (i.e., blood is not inviscid and arteries do not exhibit isotropic linear elasticity and they are not straight, uniform thickness tubes over large distances), this equation provides considerable qualitative insight. Increases in material stiffness, as in aging, and increases in wall thickness, as in

hypertension (cf. Sect. 11.1), can each lead to increased pulse wave velocity and thus clinical concern. Moreover, increasing information on structure—function relations in arterial wall mechanics suggest that many genetic mutations (e.g., those to fibrillin-1 in Marfan syndrome; cf. Observation 6.3) can similarly lead to arterial stiffening and adverse clinical outcomes. Again, therefore, there is strong motivation to understand better the coupled effects of the solid and fluid mechanics as well as the associated mechanobiological and mechanochemical effects on diverse cell types, which in arterial mechanics predominantly means smooth muscle cells, fibroblasts, and endothelial cells.

7.5 Blood Characteristics

Although the flow of air in the lungs and the flow of urine in the renal system are very important problems in biofluid mechanics, both of these fluids can be assumed to exhibit a Newtonian behavior in most cases. Indeed, the flows of physiologic salt solutions in laboratory and clinical settings can likewise be treated as Newtonian. Here, therefore, let us consider blood in more detail, both because of its central role in hemodynamics and as an illustrative non-Newtonian fluid.

7.5.1 *Plasma*

Blood is a viscous solid–fluid mixture consisting of plasma and cells. Plasma is composed of ~90 % water and contains inorganic and organic salts as well as various proteins: albumin, the globulins, and fibrinogen. Collectively, these proteins represent about 7–8 % of the plasma by weight. Albumin, the smallest plasma protein, is present in the largest concentration and represents about half of the protein mass; it has a major role in regulating the pH and the colloid osmotic pressure. The alpha and beta globulins, usually 45 % of the plasma protein mass, are antibodies that fight infection. Fibrinogen is the largest of the plasma proteins and, through its conversion to long strands of fibrin, has a major role in the process of clotting; it accounts for only about 5 % of the plasma protein mass. Serum is simply the fluid that remains after blood is allowed to clot. For the most part, the composition of serum is the same as that of plasma, with the exception that the clotting proteins, primarily fibrinogen, and platelets have been removed. As noted earlier, plasma and, thus, serum exhibit a Newtonian behavior; the viscosity of plasma, for example, is ~1.2 cP at 37 °C and its specific gravity is 1.03. For comparison, the viscosity of water is ~1.0 cP at 20 °C and ~0.7 cP at 37 °C.

7.5.2 Blood Cells

The cellular portion of blood consists of three primary types of cell: erythrocytes, leukocytes, and platelets. The most abundant of these are the erythrocytes, or red blood cells (RBCs), which constitute about 95–97 % of the cellular component of blood. This class of cells has a normal life span on average of 120 days, which corresponds to a net turnover rate of ~ 0.8 % per day. They are produced by the bone marrow and removed primarily by the spleen. Erythrocytes consist of a thin, flexible membrane with an interior filled with a hemoglobin solution; whereas the membrane can be modeled as a solid, the hemoglobin solution can be modeled as a fluid with a viscosity of ~ 6 cP. Clearly, then, there is great advantage to packaging the hemoglobin within deformable membranes rather than transporting it directly through the circulation. The major role played by the RBCs is the transport of oxygen that is bound to the hemoglobin, which constitutes about 95 % of their dry weight. Consequently, the density of a red blood cell is higher than that of plasma, and in a quiescent state, the RBCs tend to settle. This settling is used in the laboratory to determine the volume fraction of red blood cells, called the *hematocrit* and often denoted by H ; its value typically varies between 40 and 50 %.

Red blood cells in blood that is not flowing have a unique shape described as a biconcave discoid with a major diameter of approximately $7.6 \mu\text{m}$, a maximum thickness of about $2.8 \mu\text{m}$, and a minimum thickness of $1.44 \mu\text{m}$. The average human red blood cell has a volume of about $98 \mu\text{m}^3$ and a surface area of $130 \mu\text{m}^2$. There are about 5×10^6 red blood cells in a cubic millimeter of blood; hence, there is tremendous surface area available for gas exchange. When subjected to low shear rates, red blood cells can form face-to-face stacked structures called rouleaux, which, in turn, can clump together to form larger RBC structures called aggregates (Fig. 7.12). Both rouleaux and aggregates break apart under conditions of increased blood flow, or higher shear rates as noted earlier, which contributes to the pseudoplastic character of blood.

Example 7.7 The biconcave shape of the RBC increases its surface area-to-volume ratio. Compute this ratio and compare it to the value that would hold for a spherical cell.

Solution: Given the stated volume V and the surface area A of $98 \mu\text{m}^3$ and $130 \mu\text{m}^2$, respectively, we have a ratio of $1.33 \mu\text{m}^{-1}$ for the biconcave shape. If the RBC were a sphere of volume $98 \mu\text{m}^3$, then its radius would be

$$r = (3V/4\pi)^{1/3} = 2.86 \mu\text{m}.$$

The associated surface area would thus be $A = 4\pi r^2 = 103 \mu\text{m}^2$; thus, for a sphere, the ratio of surface area to volume would be $103/98 = 1.05 \mu\text{m}^{-1}$. This value is significantly less than that for the biconcave disk. Of course, in the capillary, the RBC deforms significantly from its baseline shape, which could further increase the ratio of surface area to volume, although some have suggested that the surface area tends to remain constant. A constant surface area can be accounted for constitutively for the membrane as a kinematic constraint (Humphrey 2002).

The next most abundant cell type in blood is the platelets, which constitute about 4.9 % of the cell volume. There are $(2.5\text{--}3.0) \times 10^5$ platelets per cubic millimeter of blood, with cell diameters $\sim 2.5 \mu\text{m}$ and thicknesses $\sim 0.5 \mu\text{m}$. As the name implies, they have a platelike disk shape. The platelets are major players in the coagulation of blood and thus the prevention of blood loss. The remaining 0.1 % of the cellular component of blood consists of leukocytes, or white blood cells (WBCs), which form the cellular component of the immune system. There are $(5\text{--}8) \times 10^3$ WBCs per cubic millimeter of blood in health. The three primary classes of WBCs are the monocytes (16–22 μm in diameter), granulocytes (10–12 μm in diameter), and lymphocytes (7 μm in diameter). Although much fewer in number than the RBCs, there are $\sim 37 \times 10^9$ (37 billion) WBCs circulating in the blood of a healthy adult. Because the white blood cells and platelets only constitute 5 % of the cellular component of blood, their effect on the macroscopic flow characteristics of blood is typically assumed to be negligible; that is, the non-Newtonian character of blood is controlled primarily by the hematocrit and, to a lesser degree, the fibrinogen.

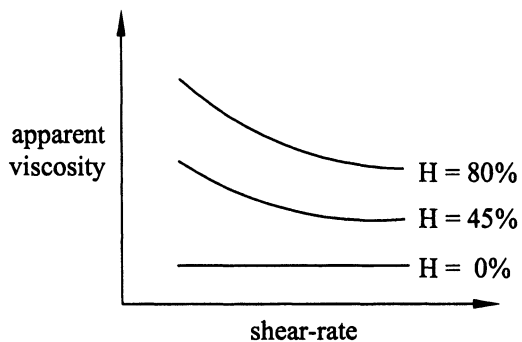
7.5.3 Additional Rheological Considerations

Rheology is a science concerned with the deformation and flow of materials. This name comes from the Greek *rheo*, meaning something that flows. Notwithstanding its non-Newtonian character, which renders blood more difficult to study than Newtonian fluids, the rheological behavior of blood is complicated further by its heterogeneous composition; that is, recall that we mentioned earlier that RBCs tend to go through capillaries in single file, with plasma between them, and, consequently, that such flows are best studied as a solid–fluid mixture. Regardless of the diameter of the vessel through which it flows, blood is always a suspension of blood cells in plasma; thus, its rheological properties depend on the concentration, mechanical properties, and interactions of its constituent parts. In particular, the rheology of blood depends strongly on the deformation of individual cells, especially the erythrocytes. For this reason, cell mechanics is as important in biofluid mechanics as it is in biosolid

mechanics (indeed, the study of the inflammatory response due to WBCs depends largely on the mechanics of their adhesion to the endothelium, thus rendering the study of leukocytes likewise important). Actually, because of the ease of isolating RBCs *in vitro*, they were among the first cells to be studied within the context of mechanics, which began in earnest in the mid- to late-1960s with the birth of modern biomechanics itself.

A marked aggregation of red blood cells at low shear rates is reflected by the yield stress τ_y , which must be exceeded for the material to flow. Many heterogeneous fluids that contain a particulate phase that forms aggregates at low shear rates exhibit a yield stress. The presence of a yield stress alone renders the behavior of a fluid non-Newtonian and, indeed, gives it an initial solidlike behavior. Materials that exhibit a yield stress but thereafter behave as a Newtonian fluid are called *Bingham plastics*—clay suspensions being a prime example. Recall that Fung's proposed constitutive equation for blood [Eq. (7.68)] accounted for both the initial yield stress and the pseudoplastic character. As noted earlier, another characteristic of a non-Newtonian behavior is that the viscosity varies with shear rate. For non-Newtonian fluids, the local slope of the stress versus shear-rate curve at a given value of the shear rate is often called the *apparent viscosity*, sometimes denoted as μ_a . The apparent viscosity of blood is shown in Fig. 7.13 as a function of hematocrit H and shear rate at a temperature of 37 °C. Consistent with its pseudoplastic character, the apparent viscosity of blood is high at low shear rates due to the presence of rouleaux and aggregates. At shear rates above about 100 s⁻¹ only individual cells exist, and blood behaves macroscopically as if it were a Newtonian fluid. Actually, blood flow in large arteries and veins is Newtonian only near the vessel wall, where the wall shear rate is significantly higher than 100 s⁻¹. As one gets closer to the centerline of the vessel, the shear rate can approach zero (shown in Chap. 9) and blood may exhibit its non-Newtonian character. Many investigators ignore this complexity and model large vessel flows assuming a constant apparent viscosity, yet we must be mindful of the actual physics in cases wherein the heterogeneity of the blood is important.

FIGURE 7.13 Viscosity of blood as a function of shear rate and hematocrit H (i.e., percentage of red blood cells by volume). The deformability and the volume fraction of red blood cells both affect the viscosity.



Whereas the erythrocytes represent the major cell species in determining the flow properties of blood in health, leukocytes, platelets, and blood-borne proteins may play significant roles in abnormal or disease conditions. Recalling that an increase of the hematocrit increases the resistance of blood to flow, note that the same effect is seen when the fibrinogen concentration is increased. Indeed, if the clotting protein fibrinogen is removed, while keeping the hematocrit unchanged, the resulting RBC suspension behaves nearly like a Newtonian fluid for shear rates as low as 0.01 s^{-1} . Fibrinogen and its effect of increasing interactions between RBCs thus appears to play a role in the non-Newtonian behavior at low shear rates; that is, the other plasma proteins, such as albumin and the globulins, do not contribute significantly to the non-Newtonian behavior of blood, although their concentration will affect the viscosity of the plasma.

Finally, it should be noted that the deformability alone (i.e., solid mechanics) of the red blood cells plays a key role in the rheology of blood. Note, therefore, that the solidlike RBC membrane is capable of moving around the fluidlike cell contents much like a tank-tread moves around the wheels of a tank. This movement of the cell membrane appears to aid the RBCs in their adapting to a flow: normal RBCs undergo shearing deformations and their long axes show a preferential alignment with flow. This clearly affects the overall rheology of blood. In diseases such as sickle cell anemia, which alters the shape and properties of the erythrocytes, one sees an associated tremendous change in the rheological properties of the blood. Indeed, the importance of RBC deformability is revealed well by studying suspensions of similarly sized but rigid spheres. The apparent viscosity of a fluid—rigid sphere solution increases nonlinearly with an increase in the volume fraction of the spheres and asymptotes near a 50 % concentration, where it ceases to flow. In comparison, blood could flow with even a 98 % hematocrit (Fung 1993). In other words, the viscosity of blood is about one-half that of a similar suspension of hard spheres.

Observation 7.3. Another fluid in the body that exhibits a strong non-Newtonian character is the *synovial fluid* in articulating joints. This fluid is secreted into the joint cavity at the synovial membrane. It is normally clear and colorless, often looking like raw egg white. Indeed, its name comes from *syn* (meaning like) and *ovial* (meaning egg). Synovial fluid is a dialysate of plasma; it contains proteins (e.g., 3.4 g/dL in pigs, including albumin and globulins), hyaluronan (119 mg/dL), and a small amount of phospholipids (19 mg/dL). The hyaluronan, which is commonly called hyaluronic acid, is the simplest glycosaminoglycan; it consists of a sequence of up to 25,000 repeating disaccharide units, and is a very large molecule (molecular weight $\sim 8 \times 10^6$). It is the hyaluronic acid that gives synovial fluid its advantageous non-Newtonian characteristics (a shear-thinning viscosity, a normal stress effect, and an elastic effect at high frequencies of loading), which can be lost in diseases such as rheumatoid arthritis. Understanding the mechanical

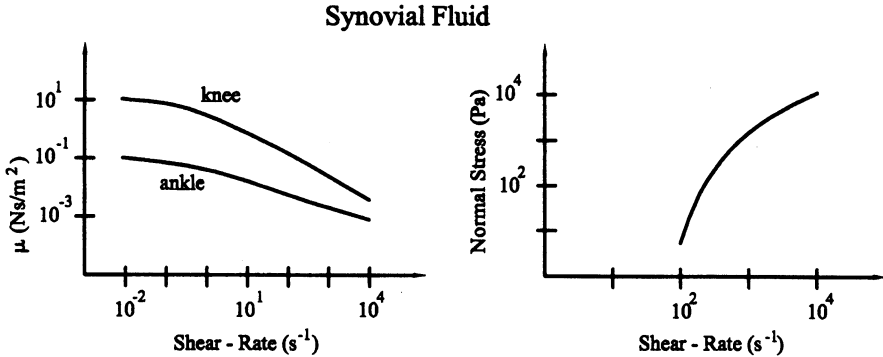


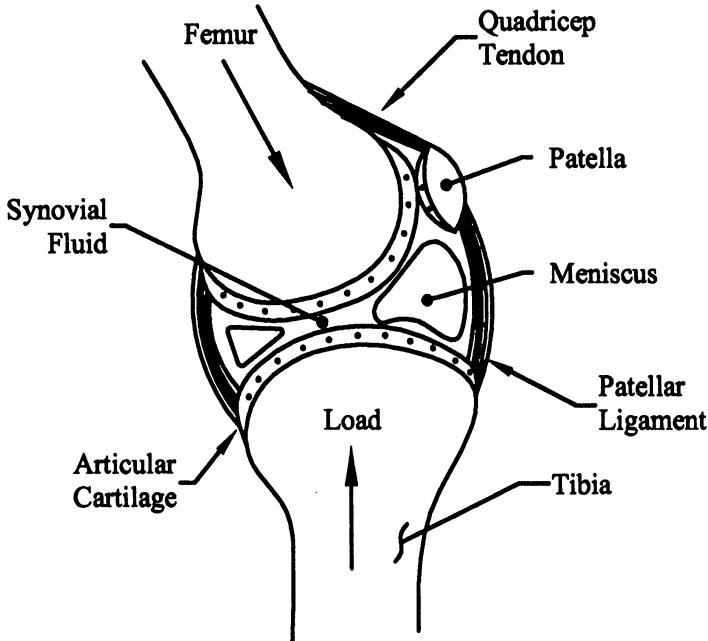
FIGURE 7.14 Shear thinning of synovial fluid, the primary lubricant in articulating joints (*left*). Another important characteristic of a non-Newtonian fluid is its ability to generate a shear-rate-dependent normal stress (*right*). Quantification of the 3-D behavior of non-Newtonian fluids is beyond an introductory text, however, and the reader is referred to Tanner (1985) for an introduction.

behavior of synovial fluid is thus important in understanding health and disease. Figure 7.14 shows the shear-thinning behavior, which is thought to be due to the increased alignment of the hyaluronic acid molecules at high shear rates.

It is commonly known that synovial fluid plays an important role as a lubricant for the relative motion of cartilage-to-cartilage in a joint such as the knee (Fig. 7.15). It is remarkable, therefore, that this is accomplished with such a small amount of synovial fluid. The human knee joint contains only 0.2 mL of synovial fluid, with a layer thickness that is typically on the order of micrometers to perhaps even nanometers. The associated coefficient of friction ranges from 0.001 to 0.03, which is remarkably small. For more on lubrication within diarthroidal joints, see Mow et al. (1990) and Chap. 5 in *Handbook of Bioengineering* edited by Skalak and Chien (1987).

7.6 Cone-and-Plate Viscometry

Recall from Chap. 3 that we derived governing differential equations for equilibrium (Sects. 3.1 and 3.2) that can be solved exactly in certain cases (Sect. 3.6). Such solutions are very valuable in biomechanics, particularly in the *design* and interpretation of experiments that are used to determine constitutive relations and likewise in the *analysis* of stress in studies of mechanotransduction. We will derive similar governing differential equations for fluids in Chap. 8 and obtain a number of exact solutions in Chap. 9. Nevertheless, in both biosolid and biofluid mechanics, much simpler approximate



The Human Knee

FIGURE 7.15 Schema of the knee showing the important constituents for geometric modeling and constitutive behavior. Cartilage and joint lubrication are considered briefly in Chap. 11.

solutions are often useful; examples include the “strength of materials solutions” for torsion and bending in Chaps. 4 and 5. Here, let us consider one such approximate solution of experimental utility in biofluid mechanics: the relationship between the viscosity of a fluid and the applied loads and geometry of a common experimental device.

A device (or meter) that measures viscosity is called a *viscometer*. There are many different types of viscometers, including the capillary viscometer, concentric cylinder viscometer, the parallel-disk viscometer, the falling-sphere viscometer, and the cone-and-plate viscometer. In each case, solutions are needed for the viscosity μ in terms of experimentally measurable quantities. A concentric cylinder viscometer is discussed in detail in Chap. 9, but here let us consider two approximate solutions. Figure 7.16 shows the so-called parallel-plate and cone-and-plate viscometers. In each case, a fluid is placed between two rigid solids: a fixed-bottom plate and an upper flat plate or a small-angle cone. Obviously, the more viscous the fluid, the more difficult it would be to rotate the upper plate or cone. One thus seeks to relate the viscosity of the fluid

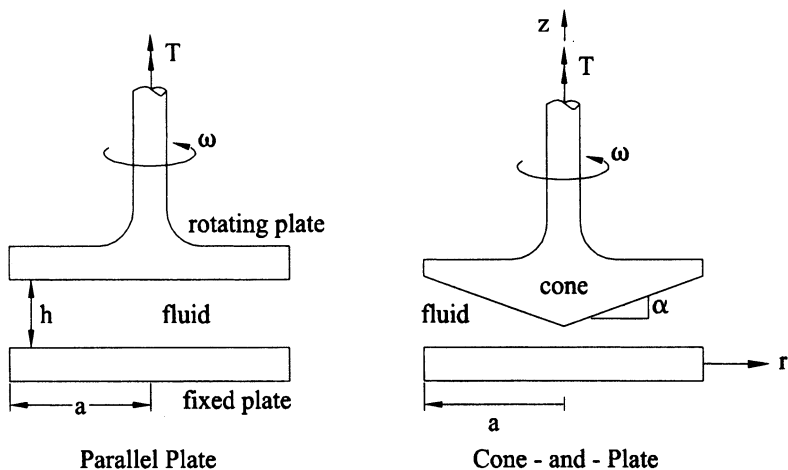


FIGURE 7.16 Schema of two “viscous-meters,” or viscometers, that are used to determine the viscosity of a fluid: the parallel-plate (*left*) and the cone-and-plate (*right*) devices.

to the applied load (torque T) and the geometry of the device (radius a , gap height h , or cone angle α) for a given constant angular velocity ω of the upper plate or cone. Although these may appear to be simple devices based on simple ideas, the generated steady-state flow field (once transients disappear due to starting the device) is at least two dimensional; the velocity will depend on both r and z . Hence, here we derive an approximate (incomplete) rather than exact (full) solution. Let us consider the cone-and-plate device. Obviously, the velocity vector of any point of the cone will have but a circumferential component, which will equal $r\omega$, where ω is the constant angular velocity; that is, the velocity is zero at the centerline and maximum at the outer edge. Let us assume, therefore, that the fluid contacting the cone will have the same velocity as the surface of the cone, namely

$$v_\theta \cong r\omega \rightarrow dv_\theta \cong \omega dr, \tag{7.73}$$

where, from geometry, $\tan \alpha = dz/dr$, and thus $dr = \cot \alpha dz$. Hence, our velocity gradient at the surface of the cone can be approximated as

$$\frac{\partial v_\theta}{\partial z} \approx \omega \cot \alpha, \tag{7.74}$$

or for small α (i.e., $\alpha \ll 1$ whereby $\cos \alpha \sim 1$ and $\sin \alpha \sim \alpha$), we have a constant shear rate

$$\frac{\partial v_\theta}{\partial z} \approx \frac{\omega}{\alpha}. \quad (7.75)$$

If we now assume a Newtonian behavior, then at the surface of the cone, we have, from Eqs. (7.58) and (7.64),

$$\sigma_{z\theta} = 2\mu \left[\frac{1}{2} \left(\frac{1}{r} \frac{\partial v_z}{\partial \theta} + \frac{\partial v_\theta}{\partial z} \right) \right]. \quad (7.76)$$

Hence, the approximate shear stress in the fluid acting on the surface of the cone is

$$\sigma_{z\theta} \approx \mu \frac{\partial v_\theta}{\partial z} = \mu \frac{\omega}{\alpha}. \quad (7.77)$$

Now, the stress on the solid, called the wall shear stress τ_w , is equal and opposite that of the fluid. It acts over a differential area on the cone, which we approximate as $dA = r d\theta dr$ for $\theta \in [0, 2\pi]$ and $r \in [0, a]$, a reasonable approximation if $\alpha \ll 1$. This wall shear stress, acting at each point over its respective cross-sectional area (i.e., $\tau_w dA$), gives rise to a differential force. The sum of all such differential forces acting at a distance r from the centerline of the device gives rise to a differential twisting moment that balances the applied torque T , which is measurable; that is [cf. Eq. (4.16)],

$$T - \int_0^a \int_0^{2\pi} r \tau_w dA = 0, \quad (7.78)$$

or

$$T = \int_0^a \int_0^{2\pi} r \left(\frac{\mu\omega}{\alpha} \right) r d\theta dr = \frac{2\pi\mu\omega}{\alpha} \int_0^a r^2 dr = \frac{2\pi\mu\omega a^3}{3\alpha}. \quad (7.79)$$

Hence,

$$\mu = \frac{3T\alpha}{2\pi\omega a^3} \quad (7.80)$$

for the cone-and-plate viscometer (Alexandrou 2001, p. 486). Clearly then, μ is “measurable” given specifications for the device (α and a) as well as measurements of the applied torque T that is required to maintain the cone at a constant angular velocity ω . Note that for a Newtonian fluid, $\mu = \text{constant}$, which is to say, T/ω would likewise be constant. If this ratio is not constant for different values of ω , the fluid is said to be non-Newtonian and μ could be estimated for

different values of the shear rate ω/α . Each value of μ so determined would be called an “apparent” viscosity. Because the viscosity of a non-Newtonian fluid varies with shear rate, the cone-and-plate device is useful because the shear rate near the surface of the cone is approximately constant ($=\omega/\alpha$). This solution is approximate (incomplete), of course, because we did not account for the no-slip boundary condition at the bottom fixed plate and we assumed that $\alpha \rightarrow 0$.

Using a similar approach, it can be shown that (Alexandrou 2001, p. 485)

$$\mu \cong \frac{2hT}{\pi\omega\alpha^4} \quad (7.81)$$

for the parallel-plate viscometer. For a description of the design of actual viscometers, see Ferry (1980, pp. 96–102). Just as in biosolid mechanics, quantification of material behavior in biofluid mechanics is fundamental to success in real-life analysis and design. It must remain a high priority in all R&D.

Chapter Summary

This Chapter is the first of four that redirects our attention to the analysis of materials that exhibit *fluidlike behaviors*, which we loosely refer to as fluids. Noting that a fluid can exist in either a liquid or gaseous form, it is generally defined as either a substance that occupies the container in which it is placed or a substance that flows in response to a shear stress, no matter how small the shear. Whereas the concept of (Cauchy) stress is the same for solidlike and fluidlike behaviors, because of the importance of “flow” in biofluid mechanics, we expanded our discussion of kinematics from displacements and strain (Chap. 2) to include *velocity* and *acceleration* (Sec. 7.3.1), *vorticity* (Sect. 7.3.2), and *rate of deformation* (Sect. 7.3.3). Because these basic kinematical concepts hold for all fluids, regardless of their constitutive behavior, they must be understood well.

We also introduced three different classes of *constitutive behaviors* for fluids. The first considered was that of a *Newtonian fluid*, that is, one exhibiting a linear relationship between stress and rate of deformation (see Fig. 7.9, with *viscosity* reflected by the slope of the linear relationship and providing a measure of the resistance to flow). Quantified via the *Navier-Poisson relations* (Eqs. (7.63)–(7.65)), the Newtonian behavior of a fluid is analogous to the Hookean behavior of a solid (i.e., a linear relation between stress and strain, with stiffness indicated by the slope of the linear relationship and providing a measure of the resistance to deformation). Nevertheless, a Newtonian behavior is not limited theoretically to particular ranges of rates of deformation and thus is more general than a Hookean behavior, which is limited to small strains.

Incorporation of the Navier-Poisson relations within linear momentum balance gives rise to the famous *Navier–Stokes equation* in fluid mechanics (Sect. 8.3), which are similarly analogous to the Navier Space Equilibrium equation in solid mechanics (Sect. 3.2). When viscous effects are negligible, the Navier-Poisson relation reduces to a constitutive relation for an *ideal fluid* (i.e., inviscid and incompressible), which gives rise to the famous Euler and Bernoulli equations of motion that are discussed in detail in Chap. 8.

Just as nonlinear constitutive relations are needed in biosolid mechanics (cf. Chap. 6), so too nonlinear relations are needed in biofluid mechanics. For example, blood at low shear rates and the synovial fluid within joints both exhibit nonlinear behaviors. Amongst the many different classes of nonlinear constitutive behaviors of fluids, we introduced a simple non-Newtonian relation in Sect. 7.4.2 wherein the viscosity depends on both an invariant measure of the rate of deformation and a threshold value of shear stress (Eqs. (7.68)–(7.70)). An illustrative solution of the flow of such a non-Newtonian fluid can be found in Sect. 9.6.

Finally, recall from the acoustic DEICE introduced in Sect. 1.7 that the formulation of a constitutive relation starts with the Delineation of general *characteristic behaviors*, which arise from the microstructural constitution of the material. Hence, we reviewed briefly the origin of blood rheology (the interested reader is again referred to books on Histology) as well as a common experimental method (cone-and-plate *viscometer*) for quantifying the constitutive response of blood (Sect. 7.6). The associated analysis is based on an approximate solution for the cone-and-plate device that depends, however, on the assumption of a Newtonian or particular non-Newtonian response, hence resulting in an expression for viscosity in terms of experimentally measurable quantities (Eq. (7.80)).

Appendix 7: Vector Calculus Review

A vector is a mathematical quantity having characteristics of magnitude and direction; a scalar is a quantity having characteristics of magnitude only. Vectors are denoted herein as boldface italics and scalars as italics. Let the vector \mathbf{u} be written in terms of its Cartesian components as $\mathbf{u} = u_x \hat{\mathbf{i}} + u_y \hat{\mathbf{j}} + u_z \hat{\mathbf{k}}$ and similarly for the vector $\mathbf{v} = v_x \hat{\mathbf{i}} + v_y \hat{\mathbf{j}} + v_z \hat{\mathbf{k}}$, where $\hat{\mathbf{i}} = (1, 0, 0)$, $\hat{\mathbf{j}} = (0, 1, 0)$, and $\hat{\mathbf{k}} = (0, 0, 1)$ are orthonormal base vectors (recall that a coordinate system is defined by its origin and a basis); that is, $(\hat{\mathbf{i}}, \hat{\mathbf{j}}, \hat{\mathbf{k}})$ are mutually orthogonal and they are of unit magnitude. We will use the caret to denote a unit magnitude in most cases [e.g., $\hat{\mathbf{w}} = \mathbf{w}/|\mathbf{w}|$, where the magnitude $|\mathbf{w}| = (\mathbf{w} \cdot \mathbf{w})^{1/2}$.]

Dot Product

The dot product between two vectors yields a scalar quantity. It can be achieved as follows:

$$\mathbf{u} \cdot \mathbf{v} = \mathbf{v} \cdot \mathbf{u} = |\mathbf{u}| |\mathbf{v}| \cos \theta, \quad (\text{A7.1})$$

where θ is the angle between \mathbf{u} and \mathbf{v} . Vectors \mathbf{u} and \mathbf{v} are orthogonal if the angle between them is $\theta = \pi/2$. Thus, \mathbf{u} and \mathbf{v} are orthogonal if and only if $\mathbf{u} \cdot \mathbf{v} = 0$. Alternatively, the dot product can be computed as

$$\begin{aligned} \mathbf{u} \cdot \mathbf{v} &= (u_x \hat{\mathbf{i}} + u_y \hat{\mathbf{j}} + u_z \hat{\mathbf{k}}) \cdot (v_x \hat{\mathbf{i}} + v_y \hat{\mathbf{j}} + v_z \hat{\mathbf{k}}) = u_x v_x (\hat{\mathbf{i}} \cdot \hat{\mathbf{i}}) + u_x v_y (\hat{\mathbf{i}} \cdot \hat{\mathbf{j}}) \\ &+ u_x v_z (\hat{\mathbf{i}} \cdot \hat{\mathbf{k}}) + u_y v_x (\hat{\mathbf{j}} \cdot \hat{\mathbf{i}}) + u_y v_y (\hat{\mathbf{j}} \cdot \hat{\mathbf{j}}) + u_y v_z (\hat{\mathbf{j}} \cdot \hat{\mathbf{k}}) \\ &+ u_z v_x (\hat{\mathbf{k}} \cdot \hat{\mathbf{i}}) + u_z v_y (\hat{\mathbf{k}} \cdot \hat{\mathbf{j}}) + u_z v_z (\hat{\mathbf{k}} \cdot \hat{\mathbf{k}}) \end{aligned} \quad (\text{A7.2})$$

Hence, it is good to remember the dot products between base vectors. For example, $\hat{\mathbf{i}} \cdot \hat{\mathbf{i}} = |\hat{\mathbf{i}}| |\hat{\mathbf{i}}| \cos \theta = (1)(1) \cos 0 = 1$. In summary,

$$\begin{aligned} \hat{\mathbf{i}} \cdot \hat{\mathbf{i}} &= 1, & \hat{\mathbf{j}} \cdot \hat{\mathbf{i}} &= 0, & \hat{\mathbf{k}} \cdot \hat{\mathbf{i}} &= 0, \\ \hat{\mathbf{i}} \cdot \hat{\mathbf{j}} &= 0, & \hat{\mathbf{j}} \cdot \hat{\mathbf{j}} &= 1, & \hat{\mathbf{k}} \cdot \hat{\mathbf{j}} &= 0, \\ \hat{\mathbf{i}} \cdot \hat{\mathbf{k}} &= 0, & \hat{\mathbf{j}} \cdot \hat{\mathbf{k}} &= 0, & \hat{\mathbf{k}} \cdot \hat{\mathbf{k}} &= 1. \end{aligned} \quad (\text{A7.3})$$

Hence, using these results in Eq. (A7.2), we see that

$$\mathbf{u} \cdot \mathbf{v} = u_x v_x + u_y v_y + u_z v_z. \quad (\text{A7.4})$$

The magnitude of a vector, say \mathbf{u} , can thus be computed as

$$|\mathbf{u}| = \sqrt{\mathbf{u} \cdot \mathbf{u}} = \sqrt{u_x^2 + u_y^2 + u_z^2}. \quad (\text{A7.5})$$

Cross Product

The cross product between two vectors yields a vector (i.e., a quantity having both a magnitude and a direction), and specifically a vector that is perpendicular to the plane containing the original two vectors. It can be written as

$$\mathbf{u} \times \mathbf{v} = -\mathbf{v} \times \mathbf{u} = |\mathbf{u}| |\mathbf{v}| \sin \theta \hat{\mathbf{e}}_{\perp}, \quad (\text{A7.6})$$

where $\hat{\mathbf{e}}_{\perp}$ is a base vector perpendicular to the plane containing \mathbf{u} and \mathbf{v} . As with the dot product, it is useful to know the cross products between the base vectors. For example, $\hat{\mathbf{i}} \times \hat{\mathbf{j}} = |\hat{\mathbf{i}}||\hat{\mathbf{j}}| \sin(\pi/2) \hat{\mathbf{k}} = \hat{\mathbf{k}}$. In summary,

$$\begin{aligned} \hat{\mathbf{i}} \times \hat{\mathbf{i}} &= \mathbf{0}, & \hat{\mathbf{j}} \times \hat{\mathbf{i}} &= -\hat{\mathbf{k}}, & \hat{\mathbf{k}} \times \hat{\mathbf{i}} &= \hat{\mathbf{j}}, \\ \hat{\mathbf{i}} \times \hat{\mathbf{j}} &= \hat{\mathbf{k}}, & \hat{\mathbf{j}} \times \hat{\mathbf{j}} &= \mathbf{0}, & \hat{\mathbf{k}} \times \hat{\mathbf{j}} &= -\hat{\mathbf{i}}, \\ \hat{\mathbf{i}} \times \hat{\mathbf{k}} &= -\hat{\mathbf{j}}, & \hat{\mathbf{j}} \times \hat{\mathbf{k}} &= \hat{\mathbf{i}}, & \hat{\mathbf{k}} \times \hat{\mathbf{k}} &= \mathbf{0}, \end{aligned} \quad (\text{A7.7})$$

Hence, the cross product for the vectors \mathbf{u} and \mathbf{v} can be computed as

$$\begin{aligned} \mathbf{u} \times \mathbf{v} &= (u_1 \hat{\mathbf{i}} + u_2 \hat{\mathbf{j}} + u_3 \hat{\mathbf{k}}) \times (v_1 \hat{\mathbf{i}} + v_2 \hat{\mathbf{j}} + v_3 \hat{\mathbf{k}}) \\ &= (\hat{\mathbf{i}} \times \hat{\mathbf{i}})(u_1 v_1) + (\hat{\mathbf{i}} \times \hat{\mathbf{j}})(u_1 v_2) + (\hat{\mathbf{i}} \times \hat{\mathbf{k}})(u_1 v_3) \\ &\quad + (\hat{\mathbf{j}} \times \hat{\mathbf{i}})(u_2 v_1) + (\hat{\mathbf{j}} \times \hat{\mathbf{j}})(u_2 v_2) + (\hat{\mathbf{j}} \times \hat{\mathbf{k}})(u_2 v_3) \\ &\quad + (\hat{\mathbf{k}} \times \hat{\mathbf{i}})(u_3 v_1) + (\hat{\mathbf{k}} \times \hat{\mathbf{j}})(u_3 v_2) + (\hat{\mathbf{k}} \times \hat{\mathbf{k}})(u_3 v_3), \end{aligned} \quad (\text{A7.8})$$

or

$$\mathbf{u} \times \mathbf{v} = (u_2 v_3 - u_3 v_2) \hat{\mathbf{i}} + (u_3 v_1 - u_1 v_3) \hat{\mathbf{j}} + (u_1 v_2 - u_2 v_1) \hat{\mathbf{k}}. \quad (\text{A7.9})$$

There is a special operator that plays a key role in fluid mechanics. Thus, recall the differential operator ∇ , also known as the *del operator*, which, relative to a Cartesian coordinate system, can be written as

$$\nabla = \hat{\mathbf{i}} \frac{\partial}{\partial x} + \hat{\mathbf{j}} \frac{\partial}{\partial y} + \hat{\mathbf{k}} \frac{\partial}{\partial z}. \quad (\text{A7.10})$$

This del operator operates on a scalar function ϕ to produce the *gradient* of ϕ , namely

$$\begin{aligned} \nabla \phi &= \left(\hat{\mathbf{i}} \frac{\partial}{\partial x} + \hat{\mathbf{j}} \frac{\partial}{\partial y} + \hat{\mathbf{k}} \frac{\partial}{\partial z} \right) \phi = \hat{\mathbf{i}} \frac{\partial \phi}{\partial x} + \hat{\mathbf{j}} \frac{\partial \phi}{\partial y} + \hat{\mathbf{k}} \frac{\partial \phi}{\partial z} \\ &= \frac{\partial \phi}{\partial x} \hat{\mathbf{i}} + \frac{\partial \phi}{\partial y} \hat{\mathbf{j}} + \frac{\partial \phi}{\partial z} \hat{\mathbf{k}}. \end{aligned} \quad (\text{A7.11})$$

Thus, the gradient of a scalar is a vector; we shall see in Chap. 8 that the “pressure gradient” plays an important role in the governing equations of motion for fluids. The del operator can also form a scalar product with a vector to produce the *divergence* of the vector:

$$\begin{aligned}\nabla \cdot \mathbf{v} &= \left(\hat{\mathbf{i}} \frac{\partial}{\partial x} + \hat{\mathbf{j}} \frac{\partial}{\partial y} + \hat{\mathbf{k}} \frac{\partial}{\partial z} \right) \cdot (v_x \hat{\mathbf{i}} + v_y \hat{\mathbf{j}} + v_z \hat{\mathbf{k}}) = \hat{\mathbf{i}} \cdot \frac{\partial}{\partial x} (v_x \hat{\mathbf{i}} + v_y \hat{\mathbf{j}} + v_z \hat{\mathbf{k}}) \\ &\quad + \hat{\mathbf{j}} \cdot \frac{\partial}{\partial y} (v_x \hat{\mathbf{i}} + v_y \hat{\mathbf{j}} + v_z \hat{\mathbf{k}}) + \hat{\mathbf{k}} \cdot \frac{\partial}{\partial z} (v_x \hat{\mathbf{i}} + v_y \hat{\mathbf{j}} + v_z \hat{\mathbf{k}}),\end{aligned}\tag{A7.12}$$

which, because $\hat{\mathbf{i}}, \hat{\mathbf{j}},$ and $\hat{\mathbf{k}}$ do not vary with position, becomes

$$\begin{aligned}\nabla \cdot \mathbf{v} &= (\hat{\mathbf{i}} \cdot \hat{\mathbf{i}}) \left(\frac{\partial}{\partial x} v_x \right) + (\hat{\mathbf{i}} \cdot \hat{\mathbf{j}}) \left(\frac{\partial}{\partial x} v_y \right) + (\hat{\mathbf{i}} \cdot \hat{\mathbf{k}}) \left(\frac{\partial}{\partial x} v_z \right) \\ &\quad + (\hat{\mathbf{j}} \cdot \hat{\mathbf{i}}) \left(\frac{\partial}{\partial y} v_x \right) + (\hat{\mathbf{j}} \cdot \hat{\mathbf{j}}) \left(\frac{\partial}{\partial y} v_y \right) + (\hat{\mathbf{j}} \cdot \hat{\mathbf{k}}) \left(\frac{\partial}{\partial y} v_z \right) \\ &\quad + (\hat{\mathbf{k}} \cdot \hat{\mathbf{i}}) \left(\frac{\partial}{\partial z} v_x \right) + (\hat{\mathbf{k}} \cdot \hat{\mathbf{j}}) \left(\frac{\partial}{\partial z} v_y \right) + (\hat{\mathbf{k}} \cdot \hat{\mathbf{k}}) \left(\frac{\partial}{\partial z} v_z \right)\end{aligned}\tag{A7.13}$$

or, by recalling the above results for dot products between the bases,

$$\nabla \cdot \mathbf{v} = \frac{\partial v_x}{\partial x} + \frac{\partial v_y}{\partial y} + \frac{\partial v_z}{\partial z}.\tag{A7.14}$$

Recall that the divergence of the velocity vector provides information on the incompressibility of a fluid flow. The del operator can also form a cross product with a vector to produce the *curl* of the vector:

$$\begin{aligned}\text{curl } \mathbf{v} &= \nabla \times \mathbf{v} = \left(\hat{\mathbf{i}} \frac{\partial}{\partial x} + \hat{\mathbf{j}} \frac{\partial}{\partial y} + \hat{\mathbf{k}} \frac{\partial}{\partial z} \right) \times (v_x \hat{\mathbf{i}} + v_y \hat{\mathbf{j}} + v_z \hat{\mathbf{k}}) \\ &= \hat{\mathbf{i}} \times \frac{\partial}{\partial x} (v_x \hat{\mathbf{i}} + v_y \hat{\mathbf{j}} + v_z \hat{\mathbf{k}}) + \hat{\mathbf{j}} \times \frac{\partial}{\partial y} (v_x \hat{\mathbf{i}} + v_y \hat{\mathbf{j}} + v_z \hat{\mathbf{k}}) \\ &\quad + \hat{\mathbf{k}} \times \frac{\partial}{\partial z} (v_x \hat{\mathbf{i}} + v_y \hat{\mathbf{j}} + v_z \hat{\mathbf{k}}),\end{aligned}\tag{A7.15}$$

which, again, simplifies considerably because the Cartesian bases do not change with position (x, y, z) . Hence,

$$\begin{aligned}\text{curl } \mathbf{v} &= (\hat{\mathbf{i}} \times \hat{\mathbf{i}}) \left(\frac{\partial}{\partial x} v_x \right) + (\hat{\mathbf{i}} \times \hat{\mathbf{j}}) \left(\frac{\partial}{\partial x} v_y \right) + (\hat{\mathbf{i}} \times \hat{\mathbf{k}}) \left(\frac{\partial}{\partial x} v_z \right) \\ &\quad + (\hat{\mathbf{j}} \times \hat{\mathbf{i}}) \left(\frac{\partial}{\partial y} v_x \right) + (\hat{\mathbf{j}} \times \hat{\mathbf{j}}) \left(\frac{\partial}{\partial y} v_y \right) + (\hat{\mathbf{j}} \times \hat{\mathbf{k}}) \left(\frac{\partial}{\partial y} v_z \right) \\ &\quad + (\hat{\mathbf{k}} \times \hat{\mathbf{i}}) \left(\frac{\partial}{\partial z} v_x \right) + (\hat{\mathbf{k}} \times \hat{\mathbf{j}}) \left(\frac{\partial}{\partial z} v_y \right) + (\hat{\mathbf{k}} \times \hat{\mathbf{k}}) \left(\frac{\partial}{\partial z} v_z \right)\end{aligned}\tag{A7.16}$$

or, by recalling the above results for cross products between the bases,

$$\begin{aligned} \text{curl } \mathbf{v} &= (\mathbf{0}) \left(\frac{\partial}{\partial x} v_x \right) + (\hat{\mathbf{k}}) \left(\frac{\partial}{\partial x} v_y \right) + (-\hat{\mathbf{j}}) \left(\frac{\partial}{\partial x} v_z \right) \\ &+ (-\hat{\mathbf{k}}) \left(\frac{\partial}{\partial y} v_x \right) + (\mathbf{0}) \left(\frac{\partial}{\partial y} v_y \right) + (\hat{\mathbf{i}}) \left(\frac{\partial}{\partial y} v_z \right) \\ &+ (\hat{\mathbf{j}}) \left(\frac{\partial}{\partial z} v_x \right) + (-\hat{\mathbf{i}}) \left(\frac{\partial}{\partial z} v_y \right) + (\mathbf{0}) \left(\frac{\partial}{\partial z} v_z \right), \end{aligned} \quad (\text{A7.17})$$

or, finally,

$$\text{curl } \mathbf{v} = \left(\frac{\partial v_z}{\partial y} - \frac{\partial v_y}{\partial z} \right) \hat{\mathbf{i}} + \left(\frac{\partial v_x}{\partial z} - \frac{\partial v_z}{\partial x} \right) \hat{\mathbf{j}} + \left(\frac{\partial v_y}{\partial x} - \frac{\partial v_x}{\partial y} \right) \hat{\mathbf{k}}. \quad (\text{A7.18})$$

Recall that the curl of the velocity is a measure of the so-called vorticity in a fluid, which provides information on the rotation of fluid elements.

Cylindricals

Because arteries, airways, ureters, medical tubing, and so forth are all cylindrical tubes, we need to be familiar with cylindrical polar coordinates. Although there are different ways to accomplish this, here we recall the relationships between cylindricals and Cartesian. Recall, therefore, that

$$x = r \cos \theta, \quad y = r \sin \theta \quad (\text{A7.19})$$

or,

$$r = \sqrt{x^2 + y^2}, \quad \theta = \tan^{-1} \left(\frac{y}{x} \right)$$

and, of course, $z = z$. Moreover,

$$\hat{\mathbf{e}}_r = \cos \theta \hat{\mathbf{i}} + \sin \theta \hat{\mathbf{j}}, \quad \hat{\mathbf{e}}_\theta = -\sin \theta \hat{\mathbf{i}} + \cos \theta \hat{\mathbf{j}}, \quad (\text{A7.20})$$

or

$$\hat{\mathbf{i}} = \cos \theta \hat{\mathbf{e}}_r - \sin \theta \hat{\mathbf{e}}_\theta, \quad \hat{\mathbf{j}} = \sin \theta \hat{\mathbf{e}}_r + \cos \theta \hat{\mathbf{e}}_\theta. \quad (\text{A7.21})$$

The latter results for $\hat{\mathbf{i}}$ and $\hat{\mathbf{j}}$ can be determined from those for $\hat{\mathbf{e}}_r$ and $\hat{\mathbf{e}}_\theta$ given the two equations for the two “unknowns.” Note, therefore, that

$$\frac{\partial \hat{\mathbf{e}}_r}{\partial \theta} = -\sin \theta \hat{\mathbf{i}} + \cos \theta \hat{\mathbf{j}} = \hat{\mathbf{e}}_\theta. \quad (\text{A7.22})$$

and, similarly,

$$\frac{\partial \hat{e}_\theta}{\partial \theta} = -\cos \theta \hat{i} - \sin \theta \hat{j} = -\hat{e}_r. \quad (\text{A7.23})$$

Conversely, \hat{e}_r and \hat{e}_θ do not vary with r .

To determine the del operator ∇ in cylindrical coordinates, recall that

$$\nabla = \hat{i} \frac{\partial(\cdot)}{\partial x} + \hat{j} \frac{\partial(\cdot)}{\partial y} + \hat{k} \frac{\partial(\cdot)}{\partial z}. \quad (\text{A7.24})$$

This relation can thus be written (using the transformations for the bases and the chain rule) as

$$\begin{aligned} \nabla = & (\cos \theta \hat{e}_r - \sin \theta \hat{e}_\theta) \left(\frac{\partial(\cdot)}{\partial r} \frac{\partial r}{\partial x} + \frac{\partial(\cdot)}{\partial \theta} \frac{\partial \theta}{\partial x} \right) \\ & + (\sin \theta \hat{e}_r + \cos \theta \hat{e}_\theta) \left(\frac{\partial(\cdot)}{\partial r} \frac{\partial r}{\partial y} + \frac{\partial(\cdot)}{\partial \theta} \frac{\partial \theta}{\partial y} \right) + \hat{e}_z \frac{\partial(\cdot)}{\partial z}. \end{aligned} \quad (\text{A7.25})$$

From Eq. (A7.19), we note that

$$\frac{\partial r}{\partial x} = \frac{1}{2}(x^2 + y^2)^{-1/2} 2x = \frac{x}{\sqrt{x^2 + y^2}} = \frac{r \cos \theta}{r} = \cos \theta \quad (\text{A7.26})$$

and, similarly (show it),

$$\frac{\partial r}{\partial y} = \sin \theta. \quad (\text{A7.27})$$

Likewise, from calculus, we recall the derivative of the arctangent; hence,

$$\frac{\partial \theta}{\partial x} = \frac{1}{1 + (y/x)^2} \left(-\frac{y}{x^2} \right) = -\frac{y}{x^2 + y^2} = -\frac{r \sin \theta}{r^2} = -\frac{\sin \theta}{r} \quad (\text{A7.28})$$

and, similarly (show it),

$$\frac{\partial \theta}{\partial y} = \frac{\cos \theta}{r}. \quad (\text{A7.29})$$

Hence, Eq. (A7.25) can be shown to become (noting that $\cos^2 \theta + \sin^2 \theta = 1$)

$$\nabla = \hat{e}_r \frac{\partial(\cdot)}{\partial r} + \hat{e}_\theta \frac{1}{r} \frac{\partial(\cdot)}{\partial \theta} + \hat{e}_z \frac{\partial(\cdot)}{\partial z}. \quad (\text{A7.30})$$

The Divergence Theorem

Let us now consider an important theorem in solid and fluid mechanics. The *divergence theorem* states that integration over an area of the dot product between a vector \mathbf{B} and an outward unit normal $\hat{\mathbf{n}}$ is equal to an integration of the divergence of \mathbf{B} over a volume:

$$\iint_{\text{Area}} \mathbf{B} \cdot \hat{\mathbf{n}} \, da = \iiint_{\text{Volume}} \nabla \cdot \mathbf{B} \, d\forall \quad (\text{A7.31})$$

wherein we use the notation \forall for volume in fluids to distinguish it from velocity, even though volume is a scalar and velocity a vector.

Example A7.1 Show numerically that the divergence theorem holds for the vector $\mathbf{B} = 4xz\hat{\mathbf{i}} - y^2\hat{\mathbf{j}} + yz\hat{\mathbf{k}}$ over a domain defined by a unit cube.

Solution: Let the six faces of the unit cube be denoted as $a, b, c, d, e,$ and f , where a is the positive x face, b is the positive y face, c is the positive z face, d is the negative x face, e is the negative y face, and f is the negative z face. Hence, note that

$$\begin{aligned} \iiint \nabla \cdot \mathbf{B} \, d\forall &= \int_0^1 \int_0^1 \int_0^1 \left(\frac{\partial B_x}{\partial x} + \frac{\partial B_y}{\partial y} + \frac{\partial B_z}{\partial z} \right) dx \, dy \, dz \\ &= \int_0^1 \int_0^1 \int_0^1 (4z - 2y + y) \, dx \, dy \, dz \\ &= \int_0^1 \int_0^1 \left[(4z - y) \int_0^1 dx \right] dy \, dz \\ &= \int_0^1 \left[4zy - \frac{y^2}{2} \right]_0^1 dz = \left[\frac{4z^2}{2} - \frac{1}{2}z \right]_0^1 = \frac{3}{2}. \end{aligned}$$

Now, by the divergence theorem, this value must equal that determined by the sum of the surface integrals:

$$\iint \mathbf{B} \cdot \hat{\mathbf{n}} \, dA = \int_a + \int_b + \int_c + \int_d + \int_e + \int_f,$$

where these integrals represent values over each of the six faces of the unit cube. Note, therefore, that

$$\begin{aligned}
 (a) \hat{\mathbf{n}} &= \hat{\mathbf{i}}, & dA &= dydz, & \text{at } x &= 1, \\
 (b) \hat{\mathbf{n}} &= \hat{\mathbf{j}}, & dA &= dx dz, & \text{at } y &= 1, \\
 (c) \hat{\mathbf{n}} &= \hat{\mathbf{k}}, & dA &= dx dy, & \text{at } z &= 1, \\
 (d) \hat{\mathbf{n}} &= -\hat{\mathbf{i}}, & dA &= dy dz, & \text{at } x &= 0, \\
 (e) \hat{\mathbf{n}} &= -\hat{\mathbf{j}}, & dA &= dx dz, & \text{at } y &= 0, \\
 (f) \hat{\mathbf{n}} &= -\hat{\mathbf{k}}, & dA &= dx dy, & \text{at } z &= 0;
 \end{aligned}$$

hence, for surface a ,

$$\int_0^1 \int_0^1 \mathbf{B} \cdot \hat{\mathbf{i}} \, dA = \int_0^1 \int_0^1 4xz|_{x=1} \, dy \, dz = 4 \left(y|_0^1 \right) \left(\frac{1}{2} z^2 \Big|_0^1 \right) = 2.$$

Similarly, show that

$$\int_b = -1, \quad \int_c = \frac{1}{2}, \quad \int_d = 0, \quad \int_e = 0, \quad \int_f = 0,$$

thus

$$\iint \mathbf{B} \cdot \hat{\mathbf{n}} \, dA = 2 - 1 + \frac{1}{2} + 0 + 0 + 0 = \frac{3}{2},$$

consistent with the volume integral and thus the divergence theorem as stated.

Exercises

- 7.1 Generate a list of 20 clinically relevant problems that demand a biofluid mechanical design or analysis.
- 7.2 Give short, concise definitions of fluid, steady flow, Eulerian approach, viscosity, Newtonian fluid, no-slip boundary condition, and convective acceleration.
- 7.3 Give short, concise definitions of fully developed flow, vorticity, laminar flow, pseudoplastic behavior, shear-rate, uniform flow, and 1-D flow.
- 7.4 Show that $\mathbf{v} \cdot \nabla \neq \nabla \cdot \mathbf{v}$ in Cartesian coordinates.
- 7.5 Show that

$$\nabla \cdot \mathbf{v} = \frac{1}{r} \frac{\partial}{\partial r} (rv_r) + \frac{1}{r} \frac{\partial v_\theta}{\partial \theta} + \frac{\partial v_z}{\partial z},$$

where

$$\nabla = \hat{e}_r \frac{\partial}{\partial r} + \hat{e}_\theta \frac{1}{r} \frac{\partial}{\partial \theta} + \hat{e}_z \frac{\partial}{\partial z}$$

in cylindrical coordinates. Likewise, show that

$$\mathbf{v} \cdot \nabla = v_r \frac{\partial}{\partial r} + \frac{v_\theta}{r} \frac{\partial}{\partial \theta} + v_z \frac{\partial}{\partial z}.$$

Hint: Recall that

$$\frac{\partial}{\partial \theta}(\hat{e}_r) = \hat{e}_\theta \quad \text{and} \quad \frac{\partial}{\partial \theta}(\hat{e}_\theta) = -\hat{e}_r.$$

7.6 Show that

$$\nabla \cdot \mathbf{v} = \frac{1}{r^2} \frac{\partial}{\partial r}(r^2 v_r) + \frac{1}{r \sin \theta} \frac{\partial}{\partial \theta}(v_\theta \sin \theta) + \frac{1}{r \sin \theta} \frac{\partial v_\phi}{\partial \phi},$$

where

$$\nabla = \hat{e}_r \frac{\partial}{\partial r} + \hat{e}_\theta \frac{1}{r} \frac{\partial}{\partial \theta} + \hat{e}_\phi \frac{1}{r \sin \theta} \frac{\partial}{\partial \phi}$$

in spherical coordinates. Hint: Recall that

$$\begin{aligned} \frac{\partial}{\partial \theta}(\hat{e}_r) &= \hat{e}_\theta, & \frac{\partial}{\partial \theta}(\hat{e}_\theta) &= -\hat{e}_r, & \frac{\partial}{\partial \phi}(\hat{e}_r) &= \sin \theta \hat{e}_\phi, \\ \frac{\partial}{\partial \phi}(\hat{e}_\theta) &= \cos \theta \hat{e}_\phi, & \text{and} & & \frac{\partial}{\partial \phi}(\hat{e}_\phi) &= -\sin \theta \hat{e}_r - \cos \theta \hat{e}_\theta. \end{aligned}$$

7.7 Consider a velocity vector $\mathbf{v} = (xt + 2y)\hat{i} + (xt^2 - yt)\hat{j}$. (a) Is this a steady flow, and why? (b) Is this a possible incompressible flow, and why? (c) Calculate the acceleration.

7.8 Compute the acceleration (in an Eulerian sense) given the following components of the velocity vector: $v_x = xt^2$, $v_y = xyt^2 + y^2$, and $v_z = 0$.

7.9 Let $\mathbf{v} = axy\hat{i} - byz\hat{j}$, with a and b known scalar constants, then (a) Calculate the acceleration vector using an Eulerian approach and (b) determine if $\nabla \cdot \mathbf{v} = 0$.

7.10 Show that $\nabla \cdot (\nabla \times \mathbf{v}) = 0$.

- 7.11 Given the velocity field $\mathbf{v} = (x + y)\hat{\mathbf{i}} + (x - y)\hat{\mathbf{j}} + 0\hat{\mathbf{k}}$, (a) determine if the flow is incompressible (i.e., $\nabla \cdot \mathbf{v} = 0$) and (b) determine if it is irrotational (i.e., $\nabla \times \mathbf{v} = \mathbf{0}$).
- 7.12 Given the following velocity field $\mathbf{v} = az^2\hat{\mathbf{i}} + bz\hat{\mathbf{k}}$. (a) Is this a possible incompressible flow (i.e., $\nabla \cdot \mathbf{v} = 0$)? (b) Is this a possible irrotational flow (i.e., $\nabla \times \mathbf{v} = \mathbf{0}$)?
- 7.13 Show that

$$\nabla \times \mathbf{v} = \left(\frac{1}{r} \frac{\partial v_z}{\partial \theta} - \frac{\partial v_\theta}{\partial z} \right) \hat{\mathbf{e}}_r + \left(\frac{\partial v_r}{\partial z} - \frac{\partial v_z}{\partial r} \right) \hat{\mathbf{e}}_\theta + \left(\frac{1}{r} \frac{\partial (rv_\theta)}{\partial r} - \frac{1}{r} \frac{\partial v_r}{\partial \theta} \right) \hat{\mathbf{e}}_z$$

in cylindrical coordinates. Hint: Note that

$$\frac{\partial v_\theta}{\partial r} + \frac{v_\theta}{r} \equiv \frac{1}{r} \frac{\partial}{\partial r} (rv_\theta).$$

- 7.14 Show that $(\mathbf{v} \cdot \nabla)\mathbf{v} = 1/2 \nabla (\mathbf{v} \cdot \mathbf{v}) - \mathbf{v} \times (\nabla \times \mathbf{v})$.
- 7.15 Derive the expressions for D_{yy} and D_{zz} .
- 7.16 Derive the expressions for D_{xz} and D_{yz} .
- 7.17 If $\mathbf{v} = v_z(r)\hat{\mathbf{e}}_z$, where

$$v_z(r) = c \left(1 - \frac{r^2}{a^2} \right)$$

and c and a are constants, determine (a) if this is a possible incompressible flow and (b) if this is a possible irrotational flow. Note that this velocity field will be shown in Chap. 9 to correspond to a steady flow in a rigid cylinder of inner radius a .

- 7.18 For the velocity field given in the previous exercise, compute D_{rr} and D_{rz} .
- 7.19 Compute $\nabla^2 \equiv \nabla \cdot \nabla$ in Cartesian coordinates.
- 7.20 Show that $\nabla^2 \mathbf{v}$ can be written in Cartesians as

$$\begin{aligned} \nabla^2 \mathbf{v} = & \left(\frac{\partial^2 v_x}{\partial x^2} + \frac{\partial^2 v_x}{\partial y^2} + \frac{\partial^2 v_x}{\partial z^2} \right) \hat{\mathbf{i}} + \left(\frac{\partial^2 v_y}{\partial x^2} + \frac{\partial^2 v_y}{\partial y^2} + \frac{\partial^2 v_y}{\partial z^2} \right) \hat{\mathbf{j}} \\ & + \left(\frac{\partial^2 v_z}{\partial x^2} + \frac{\partial^2 v_z}{\partial y^2} + \frac{\partial^2 v_z}{\partial z^2} \right) \hat{\mathbf{k}}. \end{aligned}$$

7.21 Show that in cylindricals

$$\nabla^2 = \frac{1}{r} \frac{\partial}{\partial r} \left(r \frac{\partial}{\partial r} \right) + \frac{1}{r^2} \frac{\partial^2}{\partial \theta^2} + \frac{\partial^2}{\partial z^2}$$

where ∇^2 is called the Laplacian and therefore

$$\nabla^2 \Phi = \frac{1}{r} \frac{\partial}{\partial r} \left(r \frac{\partial \Phi}{\partial r} \right) + \frac{1}{r^2} \frac{\partial^2 \Phi}{\partial \theta^2} + \frac{\partial^2 \Phi}{\partial z^2}$$

for any scalar Φ . Hint: Remember that the base vectors in cylindrical coordinates may change with direction and that

$$\nabla = \hat{e}_r \frac{\partial}{\partial r} + \hat{e}_\theta \frac{1}{r} \frac{\partial}{\partial \theta} + \hat{e}_z \frac{\partial}{\partial z}.$$

- 7.22 Sketch the change in the apparent viscosity μ_a as a function of shear rate for pseudoplastic, Newtonian, and dilatant behaviors.
- 7.23 There are about 5×10^6 RBCs/mm³ for an average human having 5 L of blood. Compute the number of RBCs circulating in the body, and if the net turnover rate is 0.8 % per day, how many cells are produced and removed per day?
- 7.24 Data from a viscometer suggest the following:

σ_{rz} (Pa)	1.7	2.7	4.8	6.5
D_{rz} (s ⁻¹)	200	300	470	600

Is this a Newtonian behavior? If not, then what type of behavior might it be?

- 7.25 According to Ethier and Simmons (2007), the inorganic content of plasma (i.e., blood minus cells) is: Na⁺ ~142 mM, K⁺ ~4 mM, Ca⁺⁺ ~2.5 mM, Mg⁺⁺ ~1.5 mM, Cl⁻ ~103 mM, HCO₃⁻ ~27 mM, phosphate (mainly HPO₄²⁻) ~1 mM, and SO₄²⁻ ~0.5 mM. Compare these values to those for a standard physiological testing solution such as Krebs or Hanks and discuss the associated implications.
- 7.26 It was shown in Sect. 7.6 that the value of the viscosity can be estimated via a cone-and-plate viscometer, namely

$$\mu = \frac{3T\alpha}{2\pi\omega a^3},$$

where T is the applied torque, α is the cone-angle, ω is the angular velocity (units of s⁻¹), and a is the maximum radius of the cone. If T_m is the maximum torque applied and $B \equiv T/T_m$, show that

$$\mu \approx 60 \frac{B}{N}$$

if $\alpha = 1.565^\circ$, $a = 2.409$ cm, and $T_m = 673.7$ dyn cm, where N is the number of revolutions per minute (rpm). Note that ω (rad/s) = $(2\pi \text{ rad/rev})(N \text{ rpm})(1 \text{ min}/60 \text{ s})$.

7.27 Given the results in Exercise 7.26 for a particular cone-and-plate viscometer, plot μ (cP) versus shear rate (s^{-1}) based on the following data:

N (rpm)	3	6	12	30	60
B	2.87	5.77	11.20	21.85	35.50

Classify the fluid (pseudoplastic, Newtonian, or dilatant) based on this plot. (Data from lecture notes by Professor D.J. Schneck, Virginia Tech.)

7.28 We will discover in Chap. 9 that the volumetric flow rate Q for a steady, incompressible flow in a rigid circular tube of radius a is given by

$$Q = \frac{\pi a^4}{8\mu} k,$$

where k is the pressure drop per unit length [i.e., $k = (P_i - P_o)/L$, where P_i and P_o are inlet and outlet pressures, respectively along the tube]. If $a \sim 1.25$ cm and $Q \sim 5$ L/min, compute the requisite percent increase in P_i (assuming P_o does not change) if $\mu = 6$ cP (hemoglobin) rather than $\mu = 3.5$ cP (whole blood). What implications would this have on the human heart with a cardiac output of 5 L/min?

7.29 Derive Eq. (7.81).

7.30 Find the gap height h for the parallel-plate viscometer in Fig. 7.16 if the torque T , the angular velocity ω , dimension a , and viscosity μ have values similar to those in Exercise 7.26.

7.31 Similar to Example A7.1, show that the divergence theorem holds for a unit cube if $\mathbf{B} = 2xy\hat{i} - 2xy\hat{j}$.